

**Review of aeronautical fatigue and structural  
integrity investigations in the UK during the period  
April 2017 - April 2019**

Hallam, D

DSTL/TR115301 Ver 1  
1 May 2019

**Dstl  
Platform Systems**

Porton Down  
Salisbury  
Wilts  
SP4 0JQ

© Crown Copyright 2019

**Release Conditions**

This document has been compiled by Dstl but contains information released by each author's organisation for presentation to the International Committee on Aeronautical Fatigue and Structural Integrity (ICAF), 2019.

## Executive summary

This review is a summary of the aeronautical fatigue and structural integrity investigations carried out in the United Kingdom during the period April 2017 to April 2019. The review has been compiled for presentation at the 36th Conference of the International Committee on Aeronautical Fatigue and Structural Integrity (ICAF), to be held in Krakow, Poland in June 2019.

The contributions generously provided by colleagues from within the aerospace industry and universities are gratefully acknowledged. The names of contributors and their affiliation are shown below the title of each item.

**Table of contents**

<b>Executive summary</b>		<b>i</b>
<b>1 Introduction</b>		<b>1</b>
<b>2 Non-destructive evaluation</b>		<b>2</b>
2.1	Development of a protocol for model-assisted qualification (MAQ).....	2
2.2	Model Assisted Qualification of Non-Destructive Inspections .....	5
2.3	Non-Contact Quantitative Delamination Assessment using Scanning Laser Vibrometry and Wavenumber Analysis.....	8
<b>3 Developments in structural health and usage monitoring</b>		<b>11</b>
3.1	The development of a practical wireless sensor based aircraft structural health monitoring system .....	11
3.2	Structural HEalth Monitoring, Manufacturing and Repair Technologies for Life Management Of Composite Fuselage (SHERLOC).....	13
3.3	Rotary-wing aircraft structural usage validation .....	16
3.4	Fixed-wing low-cost aircraft structural usage validation .....	22
<b>4 Enhancing fatigue performance</b>		<b>27</b>
4.1	Laser shock peening for life enhancement of aerospace structures .....	27
4.2	Laser shock peening activities at Cranfield University .....	30
<b>5 Guidance and fatigue performance of novel manufacturing methods</b>		<b>32</b>
5.1	Additive manufactured Ti-6Al-4V titanium under fatigue loads.....	32
5.2	UK guidance on qualification / certification of additive manufacturing in military aviation .....	36
<b>6 Corrosion management and sensing activities</b>		<b>39</b>
6.1	BEASY Corrosion Manager.....	39
6.2	Development of a structural repair and corrosion database for UK military aircraft 43	
6.3	Corrosion Sensor Development, Characterisation & Deployment.....	46
<b>7 Developments in fatigue analysis and fracture assessment tools</b>		<b>49</b>
7.1	Developments in fatigue analysis - HBM Prenscia .....	49
7.2	BEASY Fracture Assessment Tool (FASST) .....	56
7.3	A Framework to Implement Probabilistic Fatigue Design of Safe-Life Components .....	58
7.4	Rapid Calculation of Safe Acceleration Values for Aircraft Structures under Flight Test .....	61
<b>Initial distribution</b>		<b>63</b>
<b>Report documentation page v5.0</b>		<b>65</b>

## 1 Introduction

This review is a summary of the aeronautical fatigue and structural integrity investigations carried out in the United Kingdom during the period April 2017 to April 2019. The review has been compiled for presentation at the 36th Conference of the International Committee on Aeronautical Fatigue and Structural Integrity (ICAF), to be held in Krakow, Poland in June 2019.

The contributions generously provided by colleagues from within the aerospace industry and universities are gratefully acknowledged. The names of contributors and their affiliation are shown below the title of each item.

The format of the paper is similar to that of recent UK ICAF reviews; the topics covered include:

- Non-destructive evaluation
- Developments in structural health and usage monitoring
- Enhancing fatigue performance
- Guidance and fatigue performance of novel manufacturing methods
- Corrosion management and sensing activities
- Developments in fatigue analysis and fracture assessment tools

References are annotated at the end of each contribution and are self-contained within the contribution. Figure and table numbers are also self-contained within the contribution.

2 Non-destructive evaluation

2.1 Development of a protocol for model-assisted qualification (MAQ)

M. Wall, ESR Technology

2.1.1 Introduction

The high cost and long duration of experimental Probability Of Detection (POD) trials for Non Destructive Testing (NDT) technique qualification has made them impractical. Model-assisted Qualification offers a potential cost benefit by replacing certain aspects of the POD trials with theoretical models.

TWI is leading an investigation into development of a new protocol for acceptance of new NDT methods. Based on recommendations from the Military Aircraft Structures Airworthiness Advisory Group (MASAAG) this work is being carried out in conjunction with DSTL who are the project monitors and the University of Bristol who are providing aerospace NDT expertise for technical oversight of the project.

The focus of this work is to create, draft, and demonstrate a protocol for model-assisted NDT technique validation for military air-domain applications. Currently in the final year of the project, a draft release of the protocol has been developed. Figure 1 shows the condensed version. The protocol approach is primarily being demonstrated for ultrasonic inspection for metallic aerospace materials. Human factors are also being considered with a view to the final protocol providing guidance on human factors for model assisted qualification.

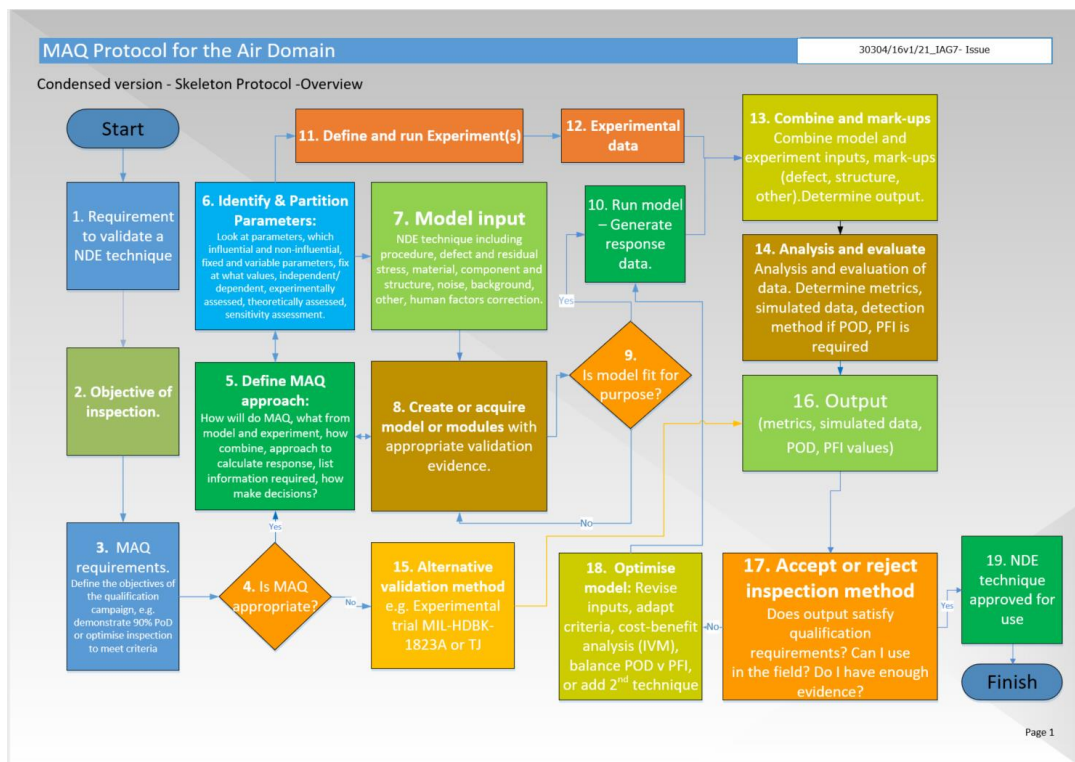


Figure 1: Current MAQ protocol - condensed version - for the air domain.

### 2.1.2 Approach (A specific case study for manual linear scan PAUT)

The protocol is being applied to the detection of cracks from fastener holes using angle-probe ultrasonic inspection, such as manual 'swivel' scanning, manual phased array sector scan and linear scans with operator-based analysis.

A specific demonstration of the protocol has been applied to manual linear scan Phased Array Ultrasound Testing (PAUT). Response data were available from previous trials at QinetiQ on a 73-notch Tornado wing section reference sample with EDM notches machined into the back of the first layer at fastener positions. For each fastener position, the corresponding rivet hole contained notches of different length and skew orientation. A case study was generated following through the steps of the protocol. A model was created in the well-established CIVA to represent the inspections carried out by QinetiQ on the 73-notch sample.

Specifically for the manual phased array linear scan, phased array delay laws were used to electronically scan along the length of the array in the same manner as was used in the experiments. A 64-element probe was modelled with pitch of 1.051mm. The probe was mounted on a wedge that was created in CIVA aiming to represent the real standoff and dimensions of the wedge that was used in the QinetiQ trials. See Figure 2.

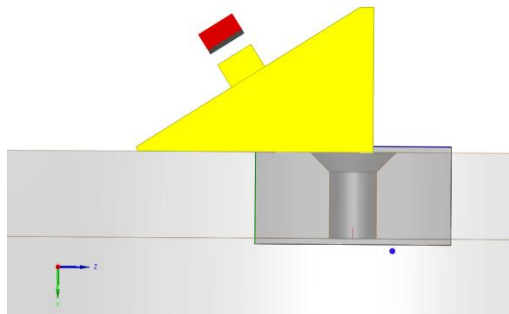


*Figure 2: CIVA simulation of the probe and wedge to represent the real standoff and dimensions of the wedge that was used.*

There were several stages of the modelling, and as it progressed it was found necessary to make certain changes to the model as per the protocol steps. The main changes were: the method of defining the geometry, the shape of flaws possible, the accuracy settings to use, and the manner in which to account for the angles between the layers, fastener and flaw. The results from the models of specific fastener geometries were compared with the relevant experimental results from the QinetiQ trials. The model was validated in the sense of being a valid computational model of the physical set-up and inspection process.

With the model being fit for purpose, the next step, was to set it up with the variable parameters being randomly sampled according to probability distributions, and to run it as a POD study instead of the deterministic models that had been run (of specific notches in the sample). The POD analysis results could have been used to support validation and acceptance of the technique however it was determined that significantly more model calculations were required than collected in order to provide

a statistically meaningful POD analysis or a POD curve, for example for a range of defect sizes.

### **2.1.3 Conclusion**

An MAQ model was successfully developed using CIVA for a specific case study demonstrating the suitability of the MAQ protocol for the manual linear PAUT inspection of cracks in fastener holes in the aluminium layer of the Tornado wing section. The model software was verified, and the model then validated against experimental peak amplitude data determined by QinetiQ from prior scans of the 73-notch reference sample.

The specific case study for manual phased array linear scan presented an assessment of the suitability of the current MAQ protocol. The main numbered boxes in the condensed MAQ protocol worked well and no changes are suggested. However, some refinement is necessary to the sub steps of the protocol in Boxes 5, 6 and 14.

### **2.1.4 Future work**

In the coming months the protocol development will be extended to Full Matrix Capture and automated phased-array scanning with automated analysis. With the protocol refined for metals the intention is also to extend and demonstrate the suitability of the protocol for large-area composite inspection. It is expected that some revision to the protocol will be necessary to take account of the considerable differences in the material and flaw morphology encountered in damaged composites. In order to ensure acceptance of the developed protocol by industry, stakeholders and interested bodies have been involved from the outset of the project. The project results will be disseminated to a wide range of stakeholders with the eventual goal to build a case for creation of a Standard.

2.2 Model Assisted Qualification of Non-Destructive Inspections

*A Ballisat, Centre for Modelling & Simulation (CFMS)*

The most common method of qualifying non-destructive inspections currently in use is through experimental trials to demonstrate that the technique is capable of repeatably finding defects of a given size. This is a costly and time-consuming process, requiring several operators and many specimens of realistic defects. The latter requirement is especially onerous – manufacturing realistic defects is notoriously difficult and obtaining examples from in-service equipment is often not possible. The increase in available desktop computing power coupled with the advent of accurate and fast models of inspections presents the opportunity to replace a significant proportion of these experimental trials with simulated results. This can significantly reduce the time and cost of qualifying an inspection.

The most common metric of inspection capability is the Probability of Detection (PoD) and the most common method of calculating this is the  $\hat{a}$  vs  $a$  method. This uses a plot of the response of the inspection ( $\hat{a}$ ) as a function of the parameter of interest ( $a$ ) to perform a linear regression and estimate the PoD. This method however assumes a linear relationship between  $\hat{a}$  and  $a$ , the response has constant normally distributed variance and that the response is not saturated. These restraints can be relaxed if a more general integral form of metric calculation is used as follows. Consider the parameter space  $\Omega$  which describes all possible combinations of all parameters that affect the inspection. Any point in this space is described by the vector  $\mathbf{x}$ . The response of the inspection given a set of parameter values is given by the function  $R(\mathbf{x})$  and the probability of this set of parameter values occurring is given by the function  $P(\mathbf{x})$ . The PoD for a parameter  $x_j$  equal to some value  $\alpha$  with a decision threshold on the response  $T$  can be calculated as

$$PoD(x_j = \alpha) = \frac{\int_{TP_{x_j=\alpha}} P(\mathbf{x}) d\mathbf{x}}{\int_{\Omega|(x_j=\alpha)} P(\mathbf{x}) d\mathbf{x}},$$

where

$$TP_{x_j=\alpha} \subset \Omega|(x_j = \alpha, R(\mathbf{x}) \geq T).$$

This approach can be generalised to any metric by redefining the condition  $TP$  to cover any decision system. This formulation requires knowledge of all possible responses of the inspection. As the number of parameters increases, the volume of the parameter space increases and it quickly becomes impractical to evaluate  $R(\mathbf{x})$  throughout  $\Omega$ . The use of sampling and interpolation has been shown to accurately map  $R(\mathbf{x})$  using of the order of hundreds of model evaluations. Latin hypercube sampling or sparse grid sampling coupled with an interpolator such as linear, radial basis function or multivariate adaptive regression splines, has been demonstrated to work well. The use of quantitative sensitivity analysis allows the relative importance of parameters to be evaluated, discounting those which have negligible impact on the response. In this work, Sobol indices are used which estimates the fraction of the total variance of the response that can be attributed to variations in each parameter and the interaction between them. This can also be used as a single, unitless metric of the reliability of the inspection as it incorporates information about the PoD and the

probability of false alarm (PFA), thus acting as a useful metric to compare disparate inspections. As this process requires knowledge of every possible outcome of the inspection, optimisation of the inspection becomes trivial and is a very beneficial by-product of this method.

These tools are best demonstrated on a canonical inspection in the aerospace domain, the inspection of cracks emanating from fastener holes in an aircraft wing skin, as shown in Fig. 1. This was modelled using Pogo FEA, an explicit time domain finite element code that uses GPUs for acceleration. Using the sampling and interpolation algorithm, a complete response map was constructed with a mean predictive error of less than 4%. This allows the metrics such as PoD and PFA to be calculated with a definition of the probability function. The sensitivity indices are summarised in Fig. 2 which shows that the position and rotation of the probe, the human factors of the inspection, are the dominant factors and that the parameter of interest, the crack length, has very little impact on the response. This shows that this inspection is very poor for inspecting fastener holes as it is very insensitive to the parameter of interest. This process required of the order of weeks to complete including model evaluation time which is a significant improvement on experiment-based qualification.

This methodology is being developed into a usable protocol for model-based qualification of inspections. This should allow these methods to become more widely used in industry, allowing novel techniques to be introduced into service faster and with reduced cost. Future work is applying these techniques to corrosion monitoring and investigating ways of encapsulating the information generated in these processes into a knowledgebase to aid future design and maintenance.

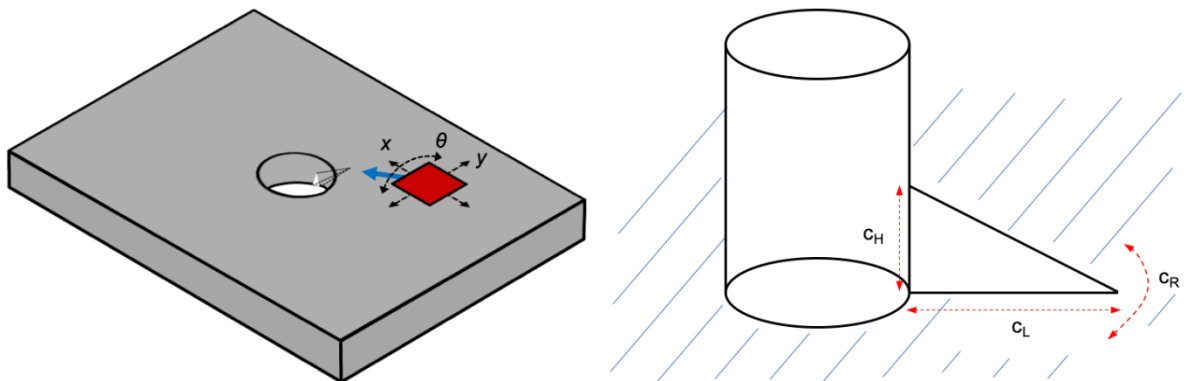


Figure 1: Diagram of the inspection of cracks emanating from a fastener hole in a wing skin.

# UK OFFICIAL

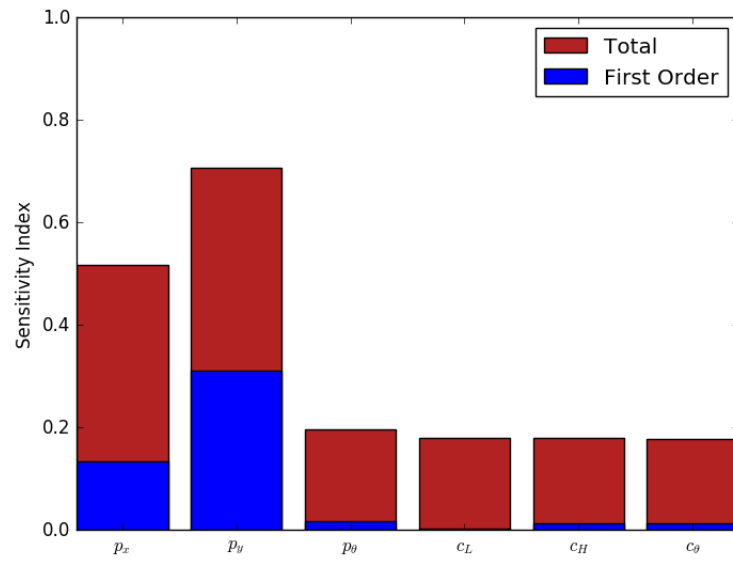


Figure 2: The sensitivity indices for the parameters of the inspection. The first order effect is a parameter's direct contribution to the variance of the response, the total index includes all interaction with other parameters.

**2.3 Non-Contact Quantitative Delamination Assessment using Scanning Laser Vibrometry and Wavenumber Analysis**

*F. Purcell, M. Eaton, M. Pearson and R. Pullin, Cardiff University*

**2.3.1 Introduction**

The challenges surrounding quickly and effectively detecting damage in composite structures are ever present. While techniques such as C-scan and phased array ultrasonic testing provide a good ability to resolve and quantify damage such as delamination they face challenges when inspection of large areas or complex geometries is required. Manually driving an ultrasonic probe over a surface requires time and a trained user. Complex geometries also call on flexible or custom probes to make good contact with the structure, further complicating the process. While the development of other NDT techniques such as thermal pulse tomography and acousto-ultrasonics have shown promise, none offer quantitative results to spatial and depth resolution on the required scale.

As guided ultrasonic waves travel through plate like structures their wavelength can be related to the frequency of the wave, material properties, wave mode and thickness. In these structures, damage such as a delamination or a disbond of a stiffener can be thought of as an effective thickness change. By pulsing a single frequency signal into a complex structure, the resulting ultrasonic waves can be captured using a laser vibrometer (LV). The captured data, which is analogous to a video of a wave passing through the structure can then be interrogated to identify changes in wavelength signifying changes in part thickness [1–3].

**2.3.2 Experimental Procedure**

To further the ability to detect damage a new approach is proposed of using mode filters in the frequency and wavenumber domain. For this technique to be used on structures of greater geometric complexity a 3D Scanning Laser Vibrometer (3DSLX) was used. To reduce scan time, improve signal to noise ratio and ensure a broad range of thicknesses were excited by a steady state frequency modulated signal ranging from 200kHz to 600kHz. A phantom was created out of 3mm thick aluminium plate with three thickness changes on the rear face of the plate as shown in Figure 1.



*Figure 1: (a) scan surface and driving PZT sensor (b) Back face of test specimen with thinning*

A lead zirconate titanate (PZT) based acoustic sensor was attached to the plate and a guided ultrasonic wave was excited. Using a 3DSLTV the response to the excitation signal was then recorded at a number of spatial sampling points separated by 1 mm.

### 2.3.3 Results and Discussion

As wavelength changes with frequency for the same thickness with in a given material filtering by wavelength would no longer give an estimation on thickness. As such a mode-based filter is proposed. Using Rayleigh-Lamb equations, which describe the relationship between plate thickness, wavelength, frequency, and material properties, a filter can be devised in the temporal and spatial frequency domain to filter the data to a specific mode and thickness. Filters were calculated at different thicknesses and applied to the data in the frequency domain. Using Monogenic signal analysis, it was then possible to determine the instantaneous amplitude at each measurement point after filtering to a specific mode. The thickness of the filter which maximised this gave the most likely thickness at each point. A thickness map for the test specimen is shown in Figure 2. The location of the thickness reductions are outlined with dashed lines.

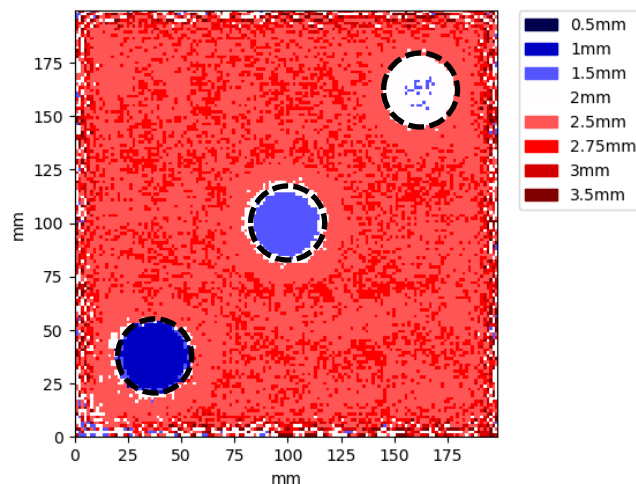


Figure 2: Thickness map based on mode filtering

The use of a 3DSLTV allows this work to be expanded to more complex geometries. This approach has been demonstrated in an aluminium structure but can be applied to composite aerospace plate like panels. Such an approach would allow a rapid inspection of large-scale structures, such as wings or fuselage panels, identifying any areas of delamination or disbond, reducing inspection times and expense whilst improving safety.

#### References:

- [1] E. B. Flynn, J. Lee, G. Jarmer, and G. Park, "Frequency-wavenumber processing of laser-excited guided waves for imaging structural features and defects," *6th Eur. Work. Struct. Heal. Monit.*, pp. 1–8, 2012.
- [2] P. D. Juarez and C. A. C. Leckey, "Multi-frequency local wavenumber analysis and ply correlation of delamination damage," *Ultrasonics*, vol. 62, pp. 56–65, 2015.

- [3] E. B. Flynn and N. D. Stull, "Toward Utilizing Full-Field Laser-Ultrasound for Practical Nondestructive Inspection with Acoustic Wavenumber Spectroscopy," in *2018 IEEE International Ultrasonics Symposium (IUS)*, 2018, pp. 1–7.

### 3 Developments in structural health and usage monitoring

#### 3.1 The development of a practical wireless sensor based aircraft structural health monitoring system

*S. Grigg, R. Pullin & C. Featherston, Cardiff University*

SENTIENT was an Innovate UK project with a consortium of eight companies involved, Cardiff University, the University of Exeter, HW Communications, Airbus, BAE Systems, TWI, NEDEAS and Ultra Electronics, each working on a certain element of the project. The aim of SENTIENT was to develop a low power wireless system capable of detecting fatigue damage growth in aircraft structures through the monitoring of Acoustic Emission.

Impact and fatigue amongst other mechanisms have the potential to cause the initiation and growth of damage during an aircraft structures' life. When this occurs energy is released in the form of ultrasonic stress waves, known as Acoustic Emission (AE). These waves propagate within the boundaries of the structure and can be detected using piezoelectric sensors (PZT's). The detection of these waves indicates the potential presence of this damage. Combining a number of these sensors in a time correlated network allows the localisation of the source of these waves through time of arrival based localisation. A large number of events coming from the same point is an indication that damage is growing in that area. In a low power system such as that being developed for SENTIENT however, accurate time correlation between sensors cannot be achieved, due to limitations in wireless clocks. A new approach has therefore been taken in which three sensors in a small triangular array which allows them to be connected to the same sensor node without excessive wiring. This triangle is able to approximate the angle of arrival of the incoming wave using trigonometry. The distance the wave has travelled can be found by using analogue frequency filtering to remove the high frequency component (S0 mode) leaving only the lower frequency, and slower, A0 mode. The difference in the arrival of these two modes is used with the known velocities to predict the distance. The developed hardware and sensor array are shown in Figure 1. A number of iterations of hardware were developed to do this and the final system consisted included data acquisition, analysis and RF comms. The power during operation was around 17mW whilst waiting for events and 40mW when transmitting data. A sleep mode of 0.33mW was also achieved.

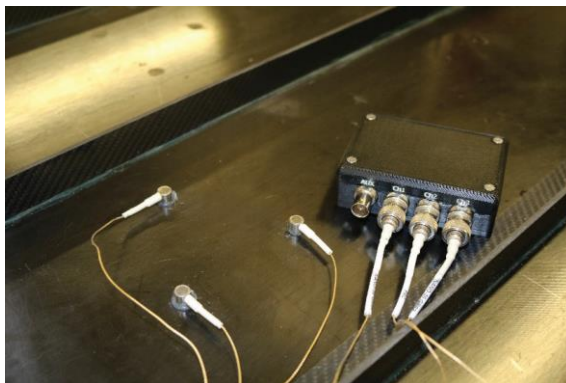


*Figure 1: Wireless sensor and Nano-30 sensors on composite panel*

This approach was tested with artificial fracture sources using the industry standard Hsu-Nielson (H-N) pencil lead breaks which replicate an AE wave originating from a fatigue crack. These tests were performed on a range of aluminium and composite structures of increasing complexity including A320 and A350 wings. A regular 100mm grid was drawn each the structure and five H-N sources created at each point. The waves were recorded using three Nano-30 sensors bonded 75mm apart and connected to the wireless sensor node which processed the received data and send the predicted location wirelessly to a laptop. The predicted error was then compared to the actual location and the error between the locations two found. Figure 1 shows the average errors for such a test on 900x900x3mm 16 ply quasi-isotropic composite panel with four 'L' stiffeners bonded to its surface.

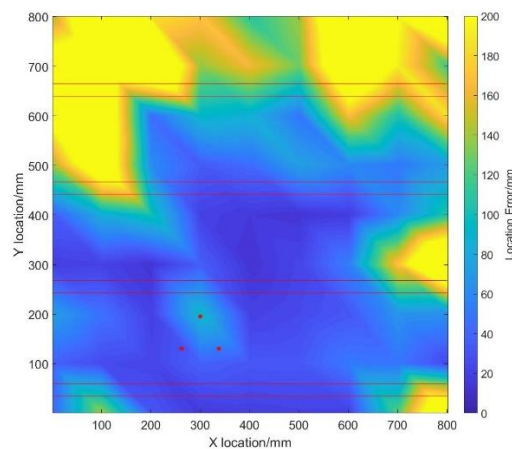


*Figure 2 – Average error map of H-N testing on a complex quasi-isotropic composite pane. Sensors indicated by red marks and stiffeners outlined in red.*

The results in Figure 2 are representative of the accuracy seen in the testing on the other panels and aircraft structures tested on. The testing highlights the presence of some significant errors however improvements can be made with further enhancements and refinement in hardware, a number of which have been identified. The results presented are precise, with a high level of repeatability which would allow maintenance engineers to target inspection areas effectively and efficiently.

For more information regarding the results of the SENTIENT project please see the thesis of S. Grigg entitled 'Development of a Wireless Structural Health Monitoring System for Aerospace Application'.

## 3.2 Structural Health Monitoring, Manufacturing and Repair Technologies for Life Management Of Composite Fuselage (SHERLOC)

*F. Aliabadi, Imperial College London*

SHERLOC is a core-partnership 7 year (2015-2022) project 10M€ funded by Cleansky II, ITD Airframe coordinated by Prof. Ferri M H Aliabadi involving 7 partners (Imperial College, Hellenic Aerospace Industry SA, Universidad Politécnica Madrid, Vrije Universiteit Brussel, Barcelona Supercomputing Centre, University of Sheffield, Element and FIDAMC). The main **four objectives** of the project SHERLOC are:

The design, manufacture and test of composite structures, following a building block approach, and of structures with bonded repairs which are equipped with a set of dedicated SHM sensors giving **reliable information** on the health of the structure. The achievement of this objective is to be assessed by comparison of SHM damage detection with that detected by other well-established NDE techniques and the evidence of destructive examinations across the full range of the testing to be conducted in the building block approach.

The development of advanced technical capabilities for making the integration of sensors in modern composite structures practical and efficient so as to facilitate industrialization and certification. This will be achieved by means of **optimization of sensor selection and positioning and by the development and evaluation of techniques for sensor placement during component manufacture**. The achievement of this objective is to be measured by conducting a detailed cost assessment of the additional manufacturing costs associated with sensor integration including all aspects of the certification process. Sensor integration costs will be an important component in the full assessment of operative costs of the SHM-equipped aircraft.

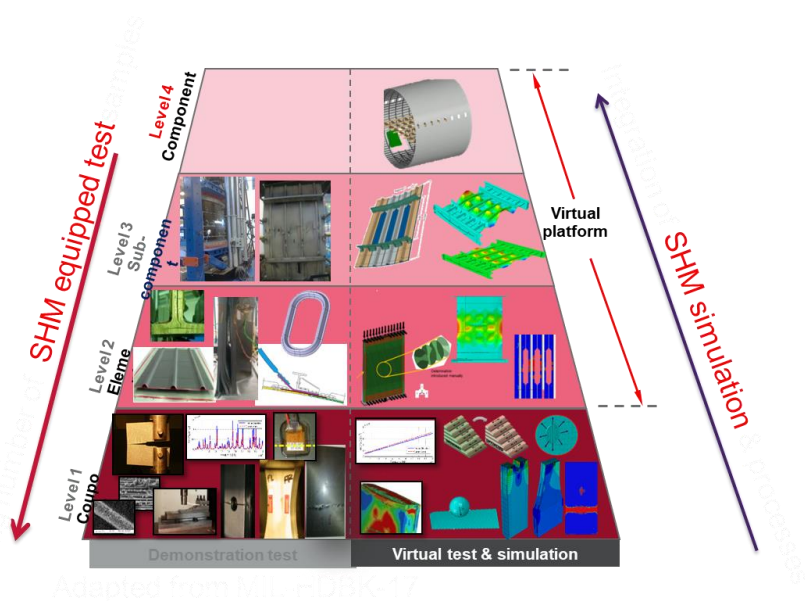
The development of a methodology that comprises of advanced large scale modelling tools, validated by structural testing, which use/process the sensor signals to **predict the residual strength** of a damaged structure at the fuselage scale of a regional aircraft. The achievement of this objective is to be assessed by evaluating the accuracy of predictions of these modelling tools through comparison with the experimental results of mechanical/structural testing across the full range of the planned building-block test programme. The verification will not only consider residual strength but also the damage mode and its progression during the failure process.

The development and experimental validation of a probabilistic method to propose a **robust design** that leads to **reduction of maintenance costs during service life and overall component cost**. The achievement of this objective is to be assessed using the full operative cost model to simulate a range of damage event scenarios for varying fleet sizes of SHM-equipped aircraft using the developed condition based maintenance approach. These operative costs will then be compared to the operative costs of current non-SHM composite aircraft using planned inspection intervals.

The on-board requirement of the SHM system will follow RTCA/DO-160C for environmental condition and test procedures of airborne equipment to ensure the durability, longevity and reliability of the installation and operation of the on-board equipment, as included in the certification guidelines.

System architecture to identify the hardware/software design considering the aircraft design criteria, the architecture of the aircraft, architecture of the aircraft support system and the cost benefits of the chosen architecture.

The SHM system maintenance should not adversely affect the performance, reliability or maintainability of the host structure.



Test Category	Environment	Certification Category
Low Temperature	-55 °C	DO-160 C 4.5.1
High Temperature	70 °C	DO-160 C 4.5.3
Thermal Shock	-55 to 70 °C at 5 °C/min	DO-160 C 5
Altitude	50,000 ft (11.6 kPa)	DO-160 C 4.6
Vibration	Random APSP 10-2000 kHz	DO-160 C 8

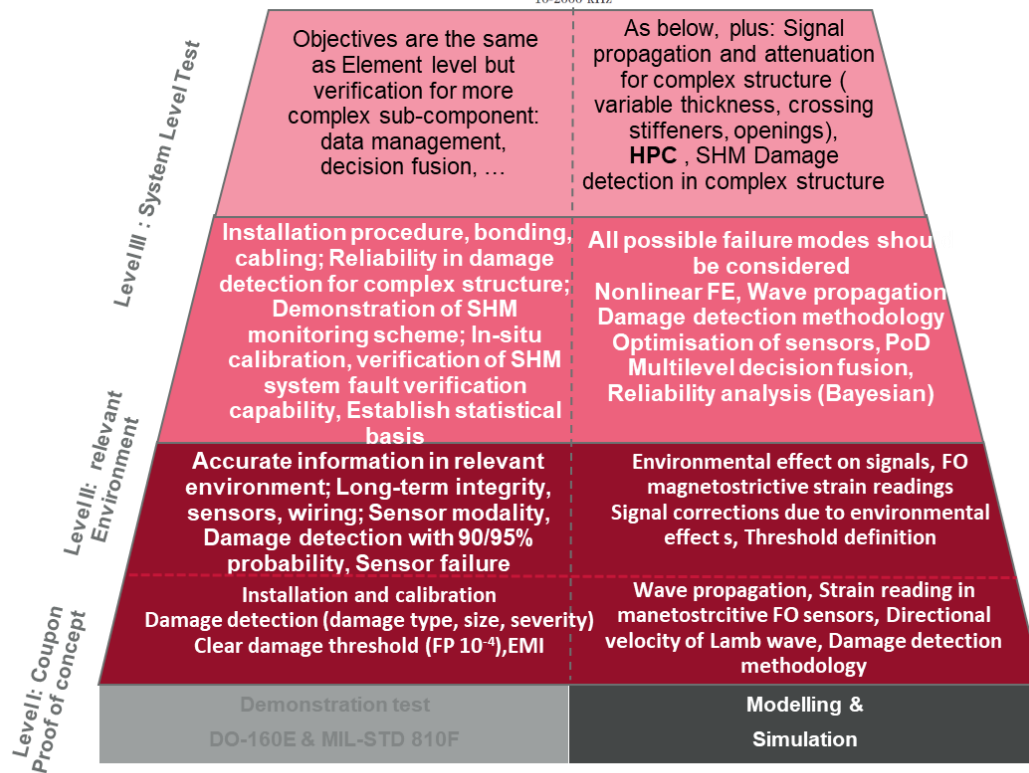


Figure 1: SHERLOC Building Block approach for SHM enabled sub-components

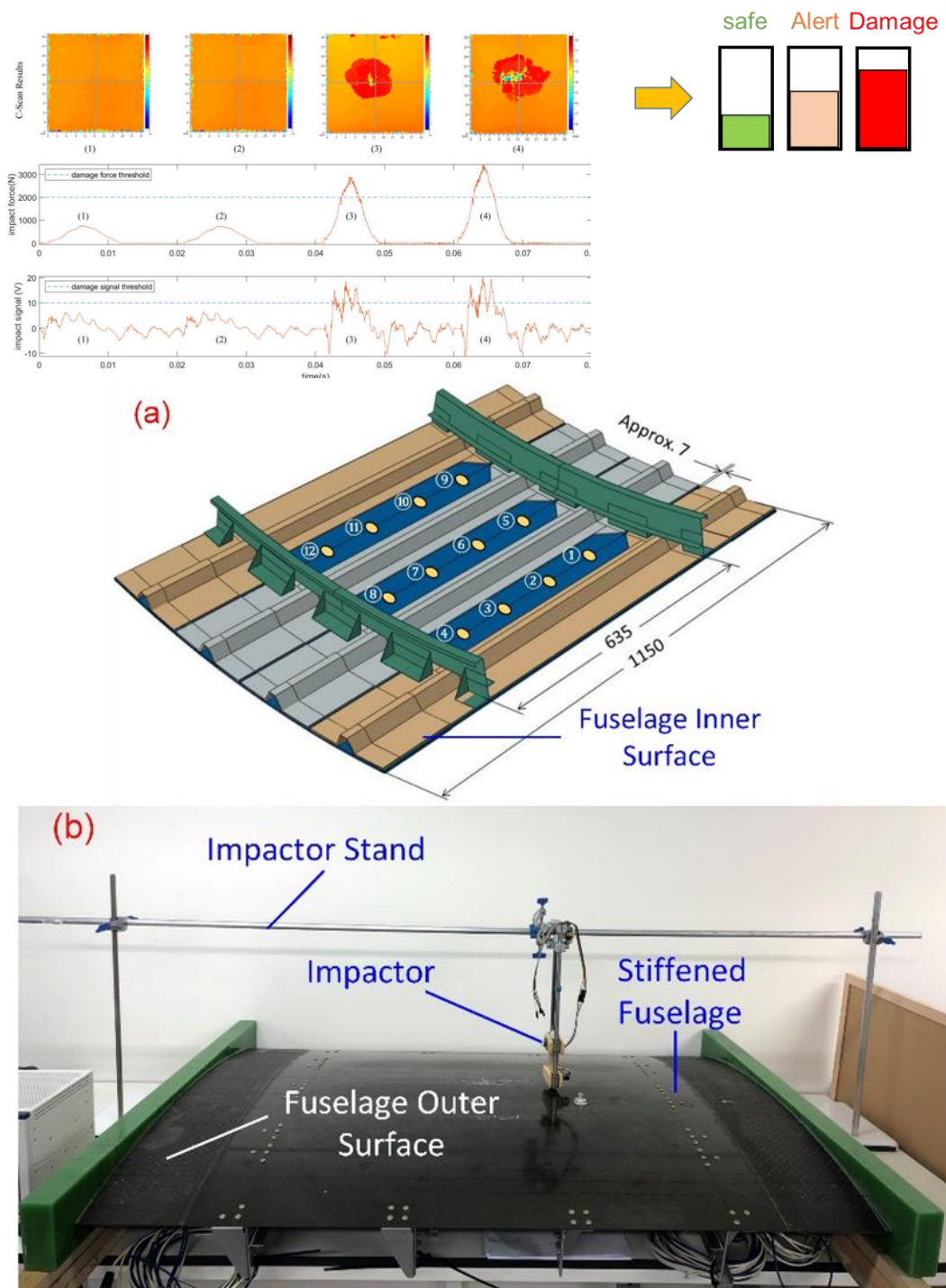


Figure 2: Laboratory validation of SHM diagnostic layer and wireless Passive sensing unit for Impact detection.

### 3.3 Rotary-wing aircraft structural usage validation

*B.H.E. Perrett<sup>1</sup> and S.C.Reed<sup>2</sup>, <sup>1</sup>Helisac, <sup>2</sup>Dstl*

The aim of this programme is to describe the usage of helicopters for comparison with Design Usage Spectra (DUS), primarily utilising a Flight Condition Recognition (FCR) approach. The aim is to use this method for Statement of Operating Intent and Usage (SOIU) validation and to cover the vast majority of an Operational Data Recording (ODR) requirement, as detailed in Military Aviation Authority Regulatory Article 5720 – Structural Integrity Management [1] and Military Aircraft Structural Airworthiness Advisory Group Paper 120 – Operational Data Recording [2].

#### 3.3.1 Wildcat

The main body of the work has been undertaken by Helisac in a collaborative programme with Leonardo Helicopters (LH) (formerly AgustaWestland), the Lynx-Wildcat MOD Delivery Team and 1710 Naval Air Squadron. Parametric data from the Health and Usage Monitoring System (HUMS)/ Flight Data Recorder (FDR), fitted to the Wildcat Flight Load Survey (FLS) aircraft and the entire service fleet, have been used to describe the flight conditions contained within the Wildcat (Figure 1) Design Usage Spectra (DUS).



*Figure 1: Wildcat helicopter (© Lee Howard)*

Refinement of the Flight Condition Recognition (FCR) algorithms (example plot at Figure 2) has been undertaken in collaboration with LH, using their definitions of the entry and exit criteria for flight conditions. A programme to use this approach to validate in-service usage of the fleet, by converting the SOI into an SOIU is underway. Over 2000 flying hours of in-service data from across all aircraft in the fleet has been input into the programme and these data have been compared with the DUS.



Figure 2: Wildcat example flight condition – transition to forward flight

**3.3.2 Puma**

A similar approach is being run in parallel on the Puma Mk2 (Figure 3) fleet, in collaboration with the MOD Puma 2 Delivery Team and Airbus Helicopters (AH).



Figure 3: Puma helicopter (© UK Crown Copyright, Image by Cpl Connor Payne)

**3.3.3 Dauphin N2**

In addition, a collaborative programme has been completed by Dstl to validate the structural, using a FCR approach, on several of the MOD Special Projects helicopter fleets.

## UK OFFICIAL

Time in flight condition and the event count were identified for the Dauphin N2 (Figure 4) Royal Navy helicopter fleet, using 400 flying hours of data from November 2016 to December 2017 [3]. The data were captured from both aircraft in the fleet instrumented with the Appareo Vision1000 data acquisition units (Figures 5 and 6).



Figure 4: Dauphin N2 helicopter (© UK Crown Copyright)



Figure 5: Appareo Vision 1000 unit

V1000 CHANNEL	ADAM ID	V1000 CHANNEL	ADAM ID
Date	DATE	Roll	ROLL
Time	TIME	RollRate	ROLLRATE
Latitude	LAT	PitchRate	PITCHRATE
Longitude	LONG	YawRate	YAWRATE
Elevation	ALT	Normal Acceleration	NZ
GroundSpeed	GS	Longitudinal Acceleration	NX
VerticalSpeed	VERTSP	Lateral Acceleration	NY
*Course	COURSE	*Slip	SLIP
Heading	HEAD	*TurnRate	TURNRATE
Pitch	PITCH		

Figure 6: Appareo Vision 1000 data captured (\* indicates calculated parameter)

A system of verification and validation of FCR was developed (Figure 7) using a combination of individual condition graphical and key parameter validation, scripted flight schedules and visual and audio flight replay (with crews announcing each event entry and exit).



Figure 7: Appareo Vision 1000 verification and validation schematic

A mechanism was also developed to differentiate between maritime (over sea) operations and over land operations. This was necessary to cater for ship-borne landings, during which the landing point may be doing 10-15kts. This is illustrated in Figure 8.

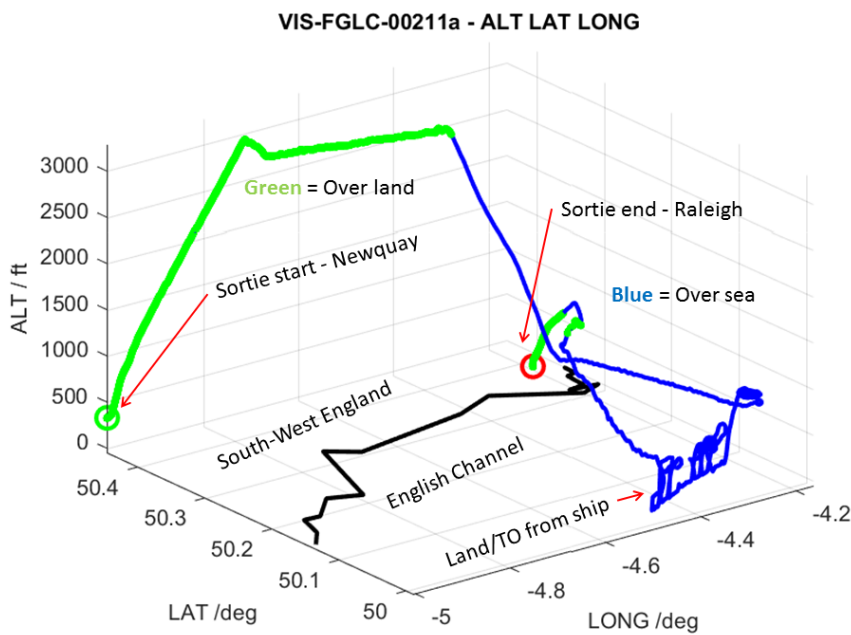


Figure 8: Schematic illustrating over land and over sea operations

### 3.3.4 Bell 412 Har2 (Griffin)

A further programme, using Flight Data Recorder (FDR) based information from the RAF Bell 412 (Griffin) HAR Mk2 aircraft, operating within 84 Squadron at RAF Akrotiri, primarily in the Search and Rescue role, has also been undertaken. The aim was to validate those aspects of usage, as defined in the Statement of Operating Intent and Usage (SOIU) that could not be validated from manual flight record data or aircrew interviews.



*Figure 9: Bell412Har2 (Griffin) helicopter using a 'Bambi' bucket for firefighting (© Ian Taylor)*

The FDR dataset, captured from two of the three aircraft in the fleet, consisted of 331 flying hours, representing 200 sorties and 621 landings. The sorties were flown between 21 January 2018 and 19 September 2018.

A detailed definition of the Flight Conditions (FC) used within the Design Usage Spectrum (DUS) was not available to Dstl. Therefore, using previous experience and available literature a FC identification rule-based system was developed, using the FDR data. This approach was based upon previous studies undertaken on the Dauphin N3, Squirrel and Dauphin N2 aircraft.

The collated output from the analysis, in terms of time in FC and discrete events was identified. Sortie Profile Codes (SPC) are not recorded for the Griffin but sortie types were identified by 84 Sqn, along with mass data, for the period of data capture. A series of recommendations were identified for consideration and this further work is currently underway.

## 3.3.5 Conclusions

The FCR approach, using a rule-based system was considered a viable system for identifying usage in accordance with [1] and [2].

Ideally this approach requires Design Organisation support to ensure FCR rules match design assumptions. If this is not possible, clearly defined and published deterministic flight conditions may be acceptable as a method of describing usage.

FDR/HUMS data set is preferable to a low-cost retro-fit system largely because of the far greater parameter set available (e.g. torque, collective position, RADALT, etc.).

Where a retro-fit (e.g. V1000) system is required, a trial installation should be undertaken for each platform type to ensure the environment is suitable for the system, in particular the vibration environment.

Where possible, FCR algorithms should be embedded within existing ground systems to support system longevity and to make maximum use of existing facilities.

## References

[1]. United Kingdom Ministry of Defence, Military Aviation Authority Regulatory Article 5720 – Structural Integrity Management, Issue 6, 31 May 2018 ([www.gov.uk](http://www.gov.uk)).

[2]. Reed, S. C., Terry, G. K. and Perrett, B. H. E., Guidance on Helicopter Operational Data Recording Programmes, Military Aircraft Structural Airworthiness Advisory Group (MASAAG) Paper 120, 27 October 2017 ([www.gov.uk](http://www.gov.uk)).

[3]. Reed, S. C., Low-cost Structural Usage Validation of Military Helicopters, in Proceedings of Addressing Analysis Challenges in a Digitally Driven World - HBM Prencia Technology Awareness Day, Sheffield, UK, 6 November 2018.

[4]. Reed, S. C., Understanding the structural usage of rotary-wing aircraft in a military environment, in the proceedings of the 29<sup>th</sup> Symposium of the International Committee on Aeronautical Fatigue and Structural Integrity (ICAF 2017), Nagoya, Japan, June 2017.

### 3.4 Fixed-wing low-cost aircraft structural usage validation

S. C. Reed, Dstl

The requirement for validation of structural usage, compared with design and qualification assumptions, is one of the cornerstones of structural integrity and is clearly regulated within the UK Ministry of Defence by the Military Aviation Authority [1], [2].

Dstl has developed a low-cost structural usage data capture system, based upon commercially-available, Micro Electro Mechanical System (MEMS) technology, for fixed-wing platforms where there is no flight data system fitted [3]. The Modular Signal Recorder (MSR) is a match-box sized self-contained unit measuring 3-axis accelerations, pressure, temperature and relative humidity and places a very low burden on front-line maintenance crews. In addition, Dstl has developed a universal Aircraft Data Analysis and Monitoring system (ADAM) for analysing flight data from a range of acquisition systems (including the MSR).

The MSR (Figure 1) has been used to capture structural usage data for the Islander and Defender (since 2011), Shadow, King Air B200/B200GT, Spitfire, Hurricane, Lancaster, Dakota, Chipmunk, Swordfish, Beaver and Hunter aircraft (also for capturing vibration data on a missile seeker head fitted to the Hunter). Road transport of Puma fuselages and naval target acquisition trials work has also been undertaken. During the latter a MSR survived a direct hit from a 0.762 round and several days in the sea thereafter. In addition, MSRs have been to measure aircraft environments for storage and in support of dehumidification trials for a range of platforms, including Typhoon aircraft.

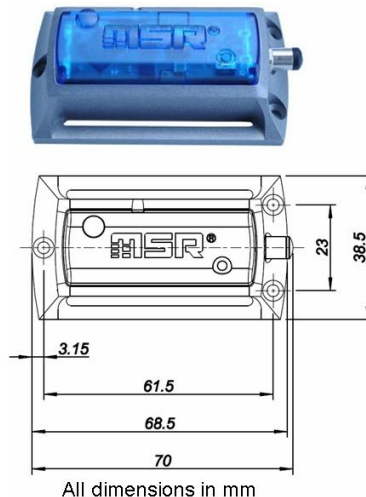


Figure 1: Modular Signal Recorder (MSR165)

#### 3.4.1 Islander and Defender

Since the last ICAF review, the MSR has remained fitted to the entire Islander and Defender fleet and has continued to capture data from these fleets (Figures 2 and 3).



Figure 2: Islander aircraft (© UK Crown Copyright)



Figure 3: Defender aircraft (© UK Crown Copyright)

### 3.4.2 Royal Navy Historic Flight Swordfish

Capture of data from the Royal Navy Historic Flight (RNHF) Swordfish (Figure 4) has continued at the 100% capture rate with all 27 flying hours / 37 sorties flown in 2017/2018 being captured and analysed. A total of 194 flying hours of Swordfish data have now been captured and analysed since 2012.



Figure 3: Swordfish aircraft W5856 (© Lee Howard)

An example normal acceleration (NZ) and estimated above ground level (AGL) time history plot for a typical Swordfish display is presented in Figure 4 below.

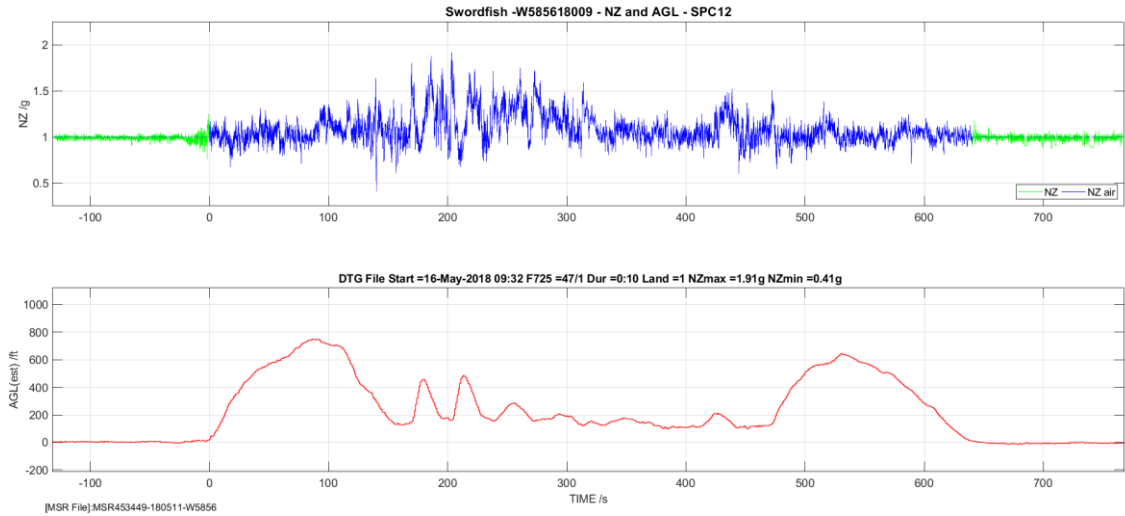


Figure 4: Swordfish display sortie time history

The NZ spectra per 100 flying hours for each year since 2012 are plotted in Figure 5. The most recent data are in identified in red on the plot. This plot is used as part of the evidence submission to confirm that the aircraft continues to be operated in a benign fashion and within its Release-to-Service limits.

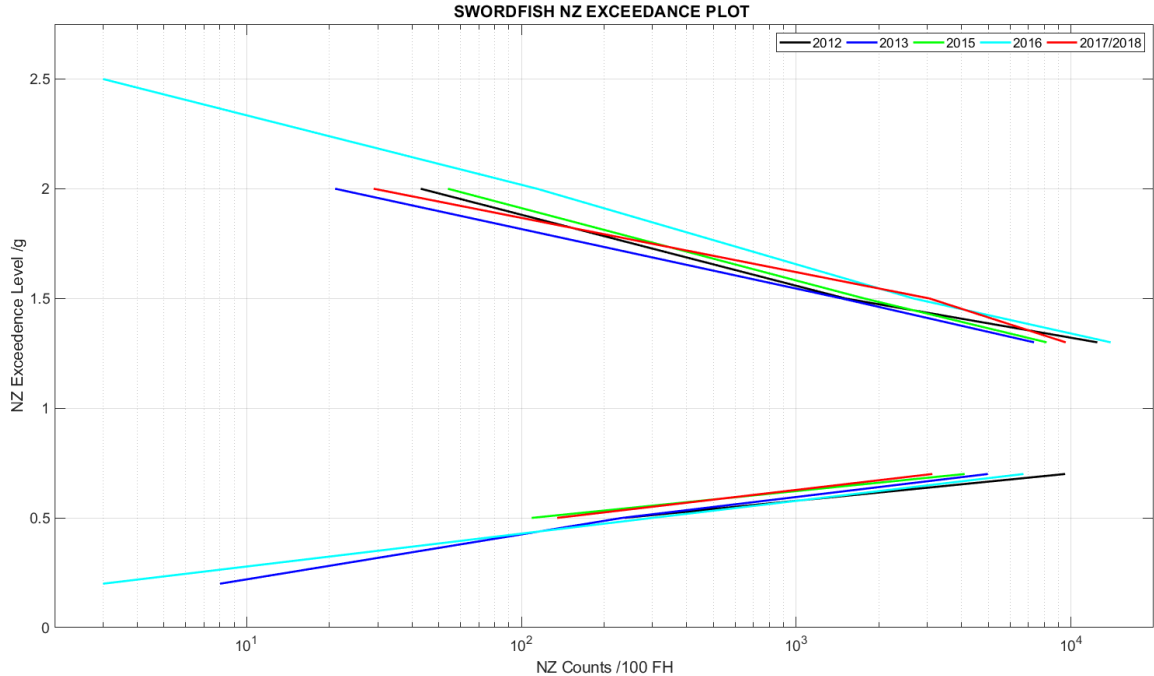


Figure 5: Swordfish NZ spectrum per 100 flying hours 2012 – 2018

### 3.4.3 Battle of Britain Memorial Flight - Spitfire, Hurricane, Lancaster, Dakota and Chipmunk

MSRs have been fitted to all aircraft in the Battle of Britain Memorial Flight (BBMF) fleet (Figure 6) for several years. Significant data sets have now been captured, for example, over 1000 flying hours of Spitfire data have been captured across the fleet over the past 4 ½ years.



*Figure 6: Battle of Britain Memorial Flight Lancaster, Spitfire and Hurricane (© UK Crown Copyright)*

Since the last ICAF review, analysis of 200 flying hours of Chipmunk data from the BBMF and RNHF fleets has been undertaken. This analysis included a range of recommendations for changes to the method for accounting for usage in the BBMF.

In addition, a rapid visualisation system (MSRtool) has been developed and deployed as an app to allow the BBMF maintenance teams to display sorties within a few minutes of the aircraft landing (usually less than the time taken to make a cup of tea!). The system is used to debrief aircrew as part of their display qualification work up and to quantify any structural exceedances rapidly. The system is fully automated from data download. An example plot (which has a linked zoom facility) is illustrated in Figure 7. Exceedances of normal operating limits are identified in red.

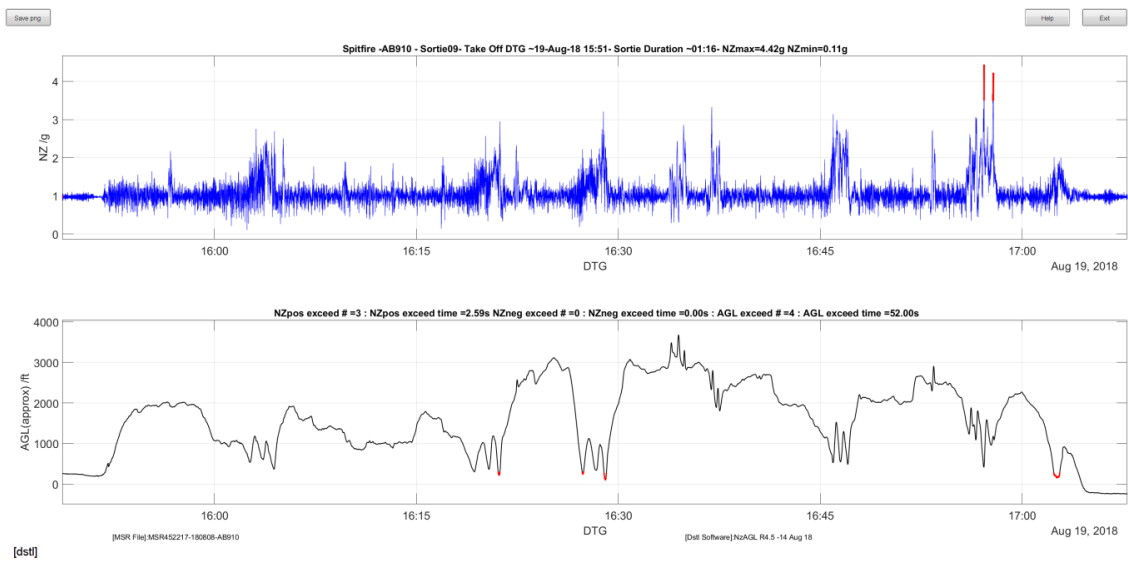


Figure 6: Battle of Britain Memorial Flight Lancaster, Spitfire and Hurricane (© UK Crown Copyright)

This MSRtool was used to analyse nearly 500 flying hours of BBMF data across the fleet for 2018 and these data have been used to review the Release-to-Service limits for the fleet.

### 3.4.4 Conclusions

The MSR, coupled with the ADAM system has proven to be an excellent and flexible ‘minimum system’ option for capturing and analysing structural usage data.

The MSR system is reliable, easy to use, low cost and low operator burden. Typical capture rates are over 90% with several fleets regularly reaching 100% capture over a full years’ flying.

The MSR analysis is time consuming and complex but enhancements, such as the MSRtool and the development of deployed apps have improved and simplified the analysis function.

### References

- [1]. United Kingdom Ministry of Defence, Military Aviation Authority Regulatory Article 5720 – Structural Integrity Management, Issue 6, 31 May 2018 ([www.gov.uk](http://www.gov.uk)).
- [2]. Reed, S. C., and Holford, D. M., Guidance for Aircraft Operational Loads Measurement Programmes, Military Aircraft Structural Airworthiness Advisory Group (MASAAG) Paper 109, 31 May 2007 ([www.gov.uk](http://www.gov.uk)).
- [3]. Reed, S. C., Low Cost Structural Usage Programmes in the proceedings of the Institution of Engineering and Technology conference Sustaining Airworthiness for Ageing Aircraft, MOD Abbey Wood, Bristol, 18 October 2017.

## 4 Enhancing fatigue performance

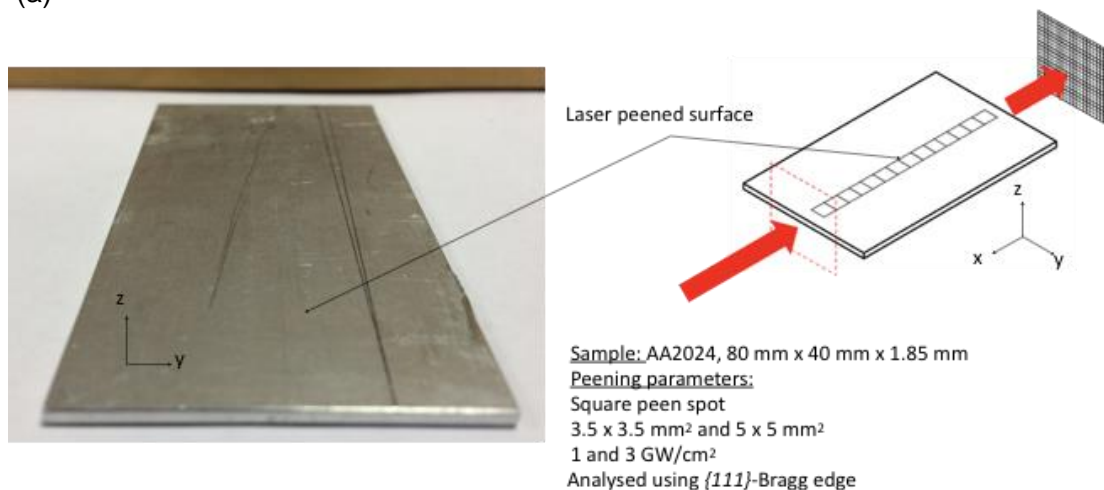
### 4.1 Laser shock peening for life enhancement of aerospace structures

*M. Fitzpatrick, N. Smyth, R. Ramadhan, M. Pavan, M. Leering, X. Zhang, Coventry University, UK*

Work within the Structural Integrity Research Group at Coventry University is studying laser shock peening as a technique to enhance the life – particularly fatigue life – of aerospace structures. We are working on advanced experimental techniques for the characterization of residual stress in components; and the direct experimental evaluation of improvement in fatigue life by the use of laser shock peening.

Recent work has involved the use of the novel neutron transmission technique for detailed mapping of the residual strain field produced by laser peening. Figure 1 shows an example of the information that can be obtained.

(a)



(b)

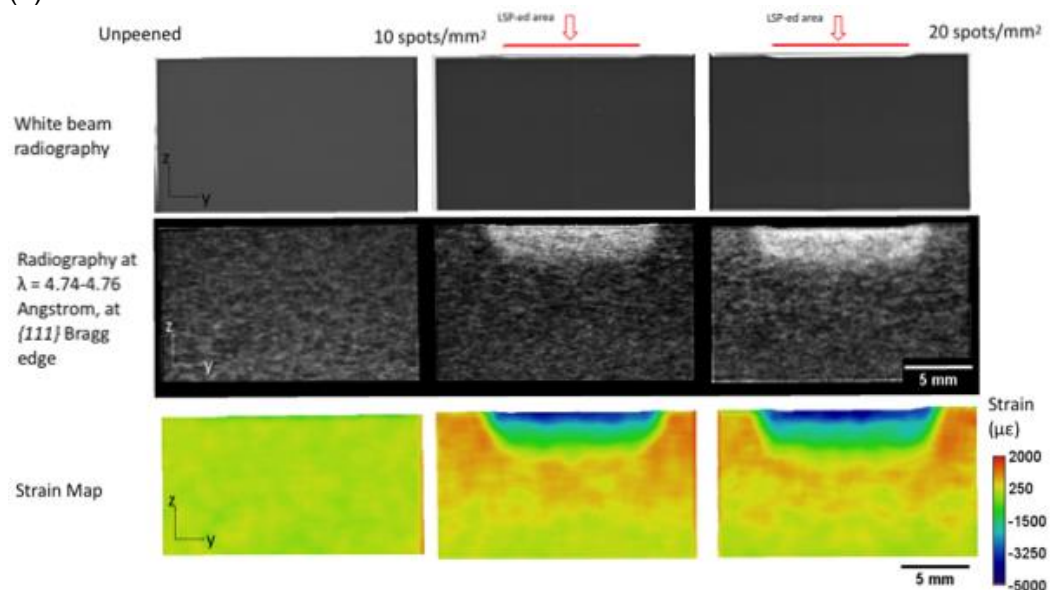


Figure 1: (a) Sample configuration. (b) Neutron transmission measurements using the IMAT instrument at the J-PARC neutron source. The top row is a radiograph of the sample, showing the depression in the LSP zone. The middle row shows the intensity of the {111} Bragg edge: the change in intensity reflects a change in the texture of the material as a consequence of the peening. The bottom row shows the residual strain map, highlighting the near-surface compression from the laser peening, balanced by tension in the depth.

We are working on establishing methods to use laser peening as a tool to retard the growth of long fatigue cracks, by the introduction of peened “patches” that will intersect the path of a growing crack. Figure 2 shows a typical configuration for fatigue testing, with patches introduced either side of the central crack-starter notch in an M(T) fatigue sample.

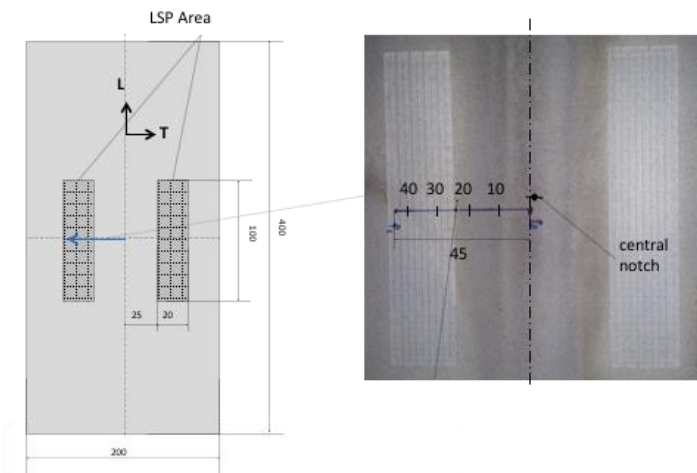


Figure 2: Sample configuration for fatigue testing

Figure 3 shows the results for different configurations, with a life improvement of up to 2.4 times depending on the width of the patches and their distance from the starter notch.

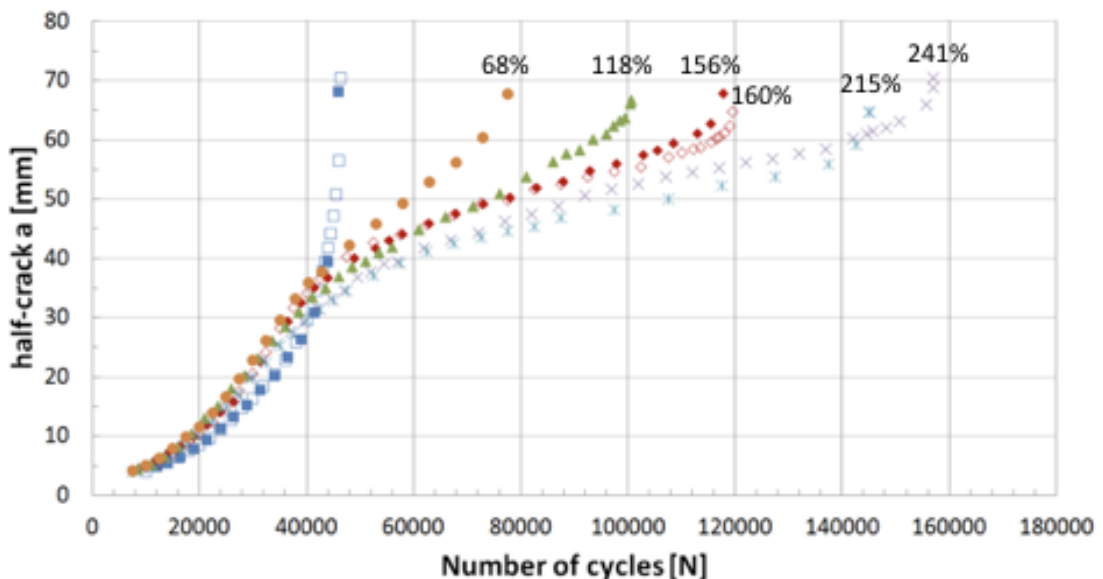


Figure 3: Crack length vs number of cycles for various peen configurations. The blue squares show the untreated condition.

### Recent relevant papers:

M. Pavan, M. E. Fitzpatrick, D. Furfari, B. Ahmed, M. Gharghour, 'Fatigue Crack Growth in a Laser Shock Peened Residual Stress Field'. *Intl J. Fatigue*. 2019:123:157-167. DOI: 10.1016/j.ijfatigue.2019.01.020

N. Smyth, M. B. Toparli, M. E. Fitzpatrick, P. E. Irving, 'Recovery of fatigue life using laser peening on 2024-T351 aluminium sheet containing scratch damage: the role of residual stress'. *Fatigue Fracture Engng Mater. Struct.* 2019:42:1161-1174. DOI: 10.1111/ffe.12981

M. B. Toparli, M. E. Fitzpatrick, 'Effect of overlapping of peen spots on residual stresses in laser peened aluminium sheets'. *Metall. Mater. Trans.* 2019:50(3):1109-12. DOI: 10.1007/s11661-018-05100-0

S. Zabeen, K. Langer, M. E. Fitzpatrick, 'Effect of alloy temper on surface modification of aluminium 2624 by laser shock peening', *Surface and Coatings Technol.* 2018:347:123-135. DOI: [doi.org/10.1016/j.surfcoat.2018.04.069](https://doi.org/10.1016/j.surfcoat.2018.04.069)

A. S. Tremsin, W. Kockelmann, J. F. Kelleher, A. M. Paradowska, R. S. Ramadhan, M. E. Fitzpatrick, 'Energy-Resolved Neutron Imaging for Reconstruction of Strain Introduced by Cold Working'. *J. Imaging*: 2018:4(3). DOI: 10.3390/jimaging4030048

R. S. Ramadhan, A. K. Syed, A. S. Tremsin, W. Kockelmann, R. Dalgliesh, B. Chen, D. Parfitt, M. E. Fitzpatrick, 'Mapping Residual Strain Induced by Cold Working and by Laser Shock Peening using Neutron Transmission Spectroscopy', *Materials and Design*:2018:143:56-64. DOI: 10.1016/j.matdes.2018.01.054

## 4.2 Laser shock peening activities at Cranfield University

*P. Irving and S. Ganguly; Cranfield University*

In the period from 2017-2019 research has continued on exploitation of the benefits to fatigue life by laser peening of 2 mm aluminium sheet and joints for fuselage applications. The work has been sponsored by Airbus and continued on previous projects which had explored the benefits of laser peening in restoration of fatigue life of 2 mm aluminium 2024-T351 after scratch and mechanical damage.

The most recent laser peening work has approached two application areas.

- (1) Benefits for damage tolerance design of the use of laser peening stripes containing local residual compressive stress located in the path of a propagating crack as crack stoppers and retarders.
- (2) To use laser peening to improve the fatigue life of bolted joints.

Project 1: Laser peened two stripes, one on each side of a propagating crack in a centre cracked panel of 2024 T-351. The cracks were grown into and across the stripes and the growth rates as the crack approached and traversed the stripes were measured. Residual stresses in the stripe were measured. It was found that as the crack approached the first stripe edge, crack acceleration due to balancing tensile stresses occurred. As the crack progressed into the stripe growth rates steadily reduced reaching a minimum about 75% of the way across. As the crack emerged from the stripe growth rates accelerated once more.

A 2D finite element model of the crack growth process was constructed for this configuration using the  $K_{\text{residual}}$  stress intensity approach to calculate the effects of residual stress variation on crack growth rates as the crack tip approached and crossed the stripe. The model was used to comprehensively explore the effects of the; magnitude of compressive residual stress through the thickness within the strip zone, geometry, length and width of the stripe and location of the stripe from the initial centre cracked notch tip on the crack growth rates and fatigue lives. It was found amongst other insights that:

- Beneficial effects on life of compressive residual stresses were partially nullified by the balancing tensile stresses encountered as the crack approached the peen stripe.
- Increasing the compressive residual stress in the stripe increased balancing tensile stresses, and the benefits to overall life were not great. Increasing stripe width was a better strategy.
- Because of stress redistribution and reduction as the crack grew, retardation and acceleration effects were most marked in the first stripe. Addition of further stripes had marginal effects on life.
- For the same reason, the closer the stripe edge was to the starting crack tip, the greater the retardation and the longer the life.

Project 2: laser peened patches of compressive stress fields were created around the holes making up a simple shear overlap bolted joint of 3 rows of 5 fasteners. The baseline unpeened fatigue lives were compared with the lives obtained on joints in

which faying surfaces had been peened according to different peening strategies where the size and shape of the peen patches had been changed. It was found that the fatigue lives of the peened samples depended on the peening strategy employed. Fatigue cracks could initiate at fastener hole edges or in fretting on the faying surfaces of the joint. Optimum fatigue lives were up to a factor of 3 better than baseline and were associated with peening strategies where compressive residual stresses inhibited fatigue crack initiation at both these locations and the improvements were not undermined by premature initiation at sites of balancing tensile residual stress.

## 5 Guidance and fatigue performance of novel manufacturing methods

### 5.1 Additive manufactured Ti-6Al-4V titanium under fatigue loads

*X. Zhang, R. Biswal, A. K. Syed, Coventry University*

In the Additive Manufacturing (AM, or 3D printing) research field, we have worked on titanium Ti-6Al-4V produced by the Wire + Arc Additive Manufacture (WAAM) process. The manufacture work was conducted by Cranfield University's Welding Engineering and Laser Processing Centre led by Professor Stewart Williams. Coventry University team has focused on the structural integrity and durability aspects. Following work has been performed over the last two years.

#### 5.1.1 High cycle fatigue and effect of porosity defects

It is recognised that the feedstock contamination may occur during the production of wire and/or during the part building process, which may lead to porosity defects [1]. Presence of defects and non-conventional microstructure will influence the fatigue performance that may limit the industrial adoption of WAAM processed materials. In this research, two types of WAAM Ti-6Al-4V walls were deposited by Cranfield University. One wall built with standard processing parameters using clean wires, resulting in fully dense or virtually no porosity condition (density 99.99%), which is denoted as the "reference wall" in this report, and the other wall built with contaminated wire to purposely produce defects in part of the wall located at the specimen gauge section area (density 99.96%), and denoted as the "porosity wall". The average size of defects was found to be  $206 \pm 80 \mu\text{m}$ . High cycle fatigue (HCF) test samples were extracted from both the reference and porosity walls. HCF testing was performed to obtain the S-N data and fatigue strength reduction factor owing to the porosity defect. In addition, interrupted fatigue-X-ray tomography experiment was also performed for observation of the porosity evolution/growth under the cyclic loads.

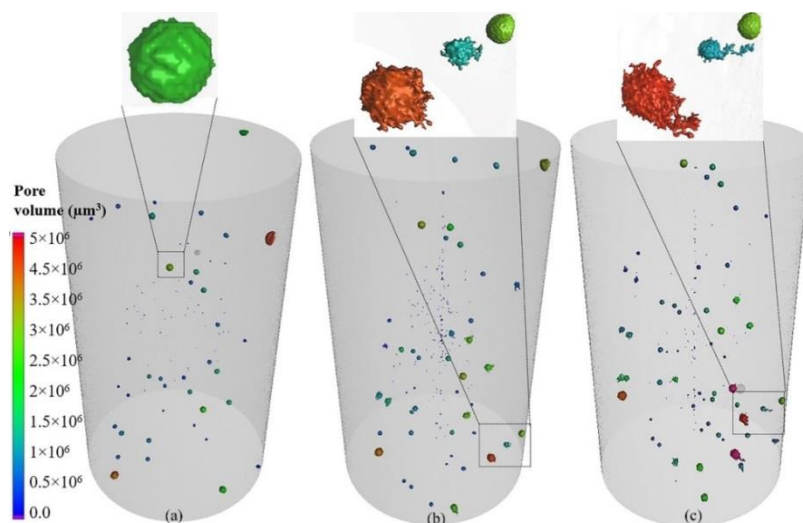


*Figure 1: Three dimensional view of X-ray computer tomography scans showing the changes in pore morphology and size with fatigue load cycles (N): (a)  $N= 0$ , (b)  $N= 2.5 \times 10^4$ , (c)  $N= 3.2 \times 10^4$  (Note: the specimen failed at 32380 cycles).*

Fig. 1 shows three dimensional view of X-ray CT scans showing the changes in pore morphology with accumulated fatigue load cycles. Fatigue loading caused change in the pore morphology from spherical to tortuous shape. Cracks initiated from sub-surface pores and propagated towards the free surface of the specimen. This can be explained by the higher value of the stress concentration factor for the sub-surface pores compared to that of the internal pores. The location of the cracks were found to be at the mid-riff section of the pores as shown in Fig. 1. Therefore, the pores were expanding in size as well as the changes in morphology.

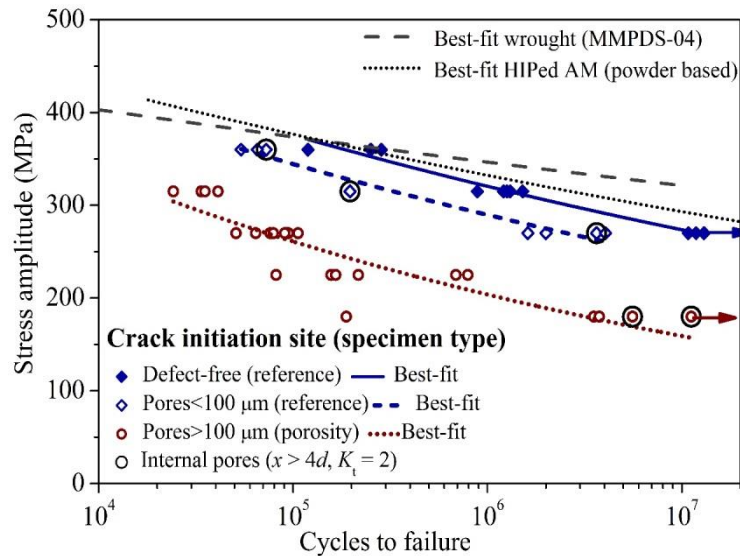


Figure 2. Fatigue test results (S-N data) at applied stress ratio 0.1 for the reference (defect free) and porosity specimens.

Fig. 2 shows the HCF test results (S-N data) for both the reference and porosity specimens. The S-N test data showed that the fatigue limit (in terms of applied stress range at 10<sup>7</sup> cycles) was 540 MPa for the reference specimen group, and 360 MPa for the porosity specimen group; all tested at an applied stress ratio of 0.1. This indicates that WAAM Ti-6Al-4V material has a notch fatigue life reduction factor of 1.5 using a notch sensitivity factor of 0.5 for spherical gas pores. Fig. 2 also shows that the fatigue performance in as-built condition (i.e. machined and polished, but no heat treatment), WAAM Ti-6Al-4V material in defect free condition was close to the traditional processed wrought material and powder bed fusion AM Ti-6Al-4V alloys in HIPed conditions.

However, there is large scatter in the S-N data in Fig. 2 for pores larger than 100 micrometres. We have found that using the applied stress alone cannot correlate the fatigue life when porosity size is greater than 100 micrometres.

Since the applied stress and defect size both play an important role in determining the fatigue strength, the stress intensity factor (SIF) range was used to correlate the fatigue test results. According to Murakami's model [2], a spherical gas pore can be treated as a planar crack of size equal to the square root of the projected area of the pore. Stress intensity factor range was calculated by Murakami's equation as shown in Eq. (1).

$$\Delta K = C \times \Delta\sigma \sqrt{\pi \sqrt{area}} \quad \text{Eq (1)}$$

where  $\Delta K$  is the stress intensity factor range,  $\Delta\sigma$  the applied stress range,  $\sqrt{area}$  the square root of the projected area of the pore, and parameter  $C$  is 0.5 for internal defects and 0.65 for surface defects. The S-N data presented in Fig. 2 have been re-plotted as a relation of  $\Delta K$  vs.  $N$  in Fig. 3 showing a much better correlation between the fatigue life and the fracture mechanics parameter, with much smaller scatters.

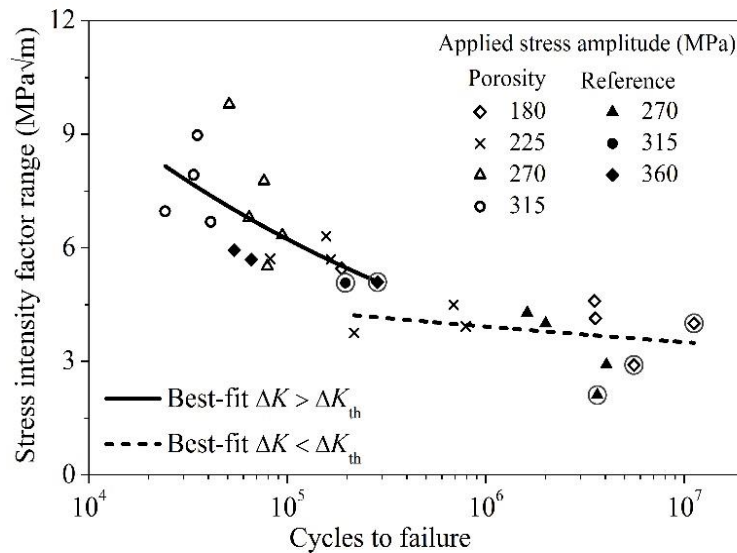


Figure 3. Correlation between fatigue life and stress intensity factor range (SIF range) for porosity defects (SIF range is calculated using the Murakami's equation, Eq. 1). Note: encircled data points denote crack initiation from internal pores; majority tests had crack initiation from sub-surface pores.

### 5.1.2 Fatigue crack growth rates

In our previous study [3] we have shown that fatigue crack growth rate was slower in single bead build WAAM Ti-6Al-4V when crack propagated across the build layers comparing to crack growing parallel to the layers. In this study we have investigated fatigue crack growth rate in parallel path and oscillation build WAAM Ti-6Al-4V. These two build strategies and the single path build used in the previous research [3] are shown in Fig. 4a. Fatigue crack growth tests were performed with a maximum load of 3 kN and a load ratio of 0.1. The results are presented in Figs. 4b and 4c compared with the single bead strategy used in the previous research [3].

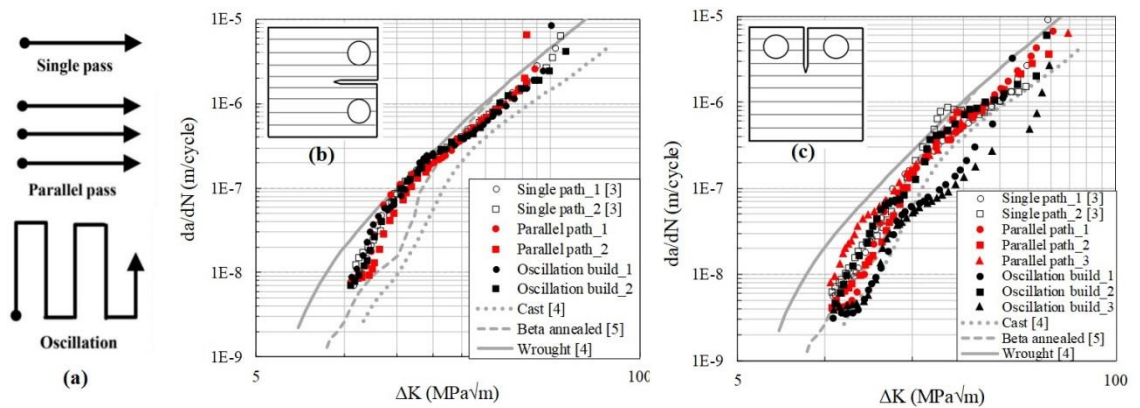


Figure 4. (a) Deposition strategies used to build WAAM Ti-6Al-4V. Fatigue crack growth rates and influence of crack orientation: (b) crack parallel to layers, (c) crack across layers.

Key findings are: (1) fatigue crack growth rate in WAAM Ti-6Al-4V is slower than a reference wrought material, but faster than cast and  $\beta$  annealed conditions; (2) for the oscillation build, crack growth rate is direction dependent, i.e. crack growing across to the layers showed lower crack growth rate compared to crack parallel to the layers due to continuous interaction of the crack tip with the layer bands along the build direction; (3) for the parallel path build, crack growth rates are very similar between the two major crack directions; can be considered as isotropic property.

## References

1. Wang, F., Williams, S., Colegrove P., AntonySAM A.A., (2013) Microstructure and mechanical properties of wire and arc additive manufactured Ti-6Al-4V, Metallurgical and Materials Transactions A: Physical Metallurgy and Materials Science, 44(2), pp. 968–977.
2. Y. Murakami, Metal fatigue: Effects of Small Defects and Nonmetallic Inclusions, 1st ed., Elsevier, 2002.
3. Zhang X., Syed, AK., Martina F., Ding J., Williams SW. Fatigue and Damage Tolerance Performance of Additive Manufactured Titanium: Control of residual stress and development of life evaluation method. Accept for presentation at ICAF2017, June 2017.
4. MMPDS hand book, SAE international, 2012.
5. Jeong D., Kwon Y., Goto M., Kimet S., (2017). High cycle fatigue and fatigue crack propagation behaviours of  $\beta$ -annealed Ti-6Al-4V alloy, International Journal of Mechanical and Materials Engineering, 12 pp. 1–10.

## 5.2 UK guidance on qualification / certification of additive manufacturing in military aviation

*M. Lunt and R. Mangham, Defence Science and Technology Laboratory (Dstl)*

### Overview

Aircraft on the UK's military register are regulated by the Military Aviation Authority (MAA), which is an independent organisation, empowered by charter by the Secretary of State for Defence, to ensure the safe design and use of military air systems. It draws on expertise from advisory groups of military, civilian and industrial experts that cover aircraft structures, systems and propulsion. The Military Aircraft Structures Airworthiness Advisory Group (MASAAG) recently commissioned a Guidance Note on the Qualification and Certification of Additive Manufactured (AM) Parts for Military Aviation, the better to advise all stakeholders on the safe exploitation of the technology. The note was published in October 2018 and is available on the MASAAG website<sup>1</sup>.

The paper covers metallic parts for aircraft structures (Grade A parts) and engines (Critical parts); non-metallic parts and aircraft systems have not been specifically addressed. Within the paper, the existing military and civil regulatory material, relevant to AM parts, has been reviewed (Chapters 3 and 4). In addition, a significant proportion of the paper has been devoted to describing the various methodologies used for AM part design and build (Chapter 5). This has been included to explain the sources of variation in performance of AM parts and to underpin the recommendations made to minimise, measure and account for these performance variations. Where appropriate, existing standards for AM or other relevant manufacturing or test methods have been identified and are referenced within this paper. The paper can be seen as the coming together of the MOD's regulatory framework and the specifics of AM metallurgy / process engineering (Figure 1).

---

1

[https://assets.publishing.service.gov.uk/government/uploads/system/uploads/attachment\\_data/file/750387/MASAAG\\_Paper\\_124.pdf](https://assets.publishing.service.gov.uk/government/uploads/system/uploads/attachment_data/file/750387/MASAAG_Paper_124.pdf) [accessed 05 March 2019]

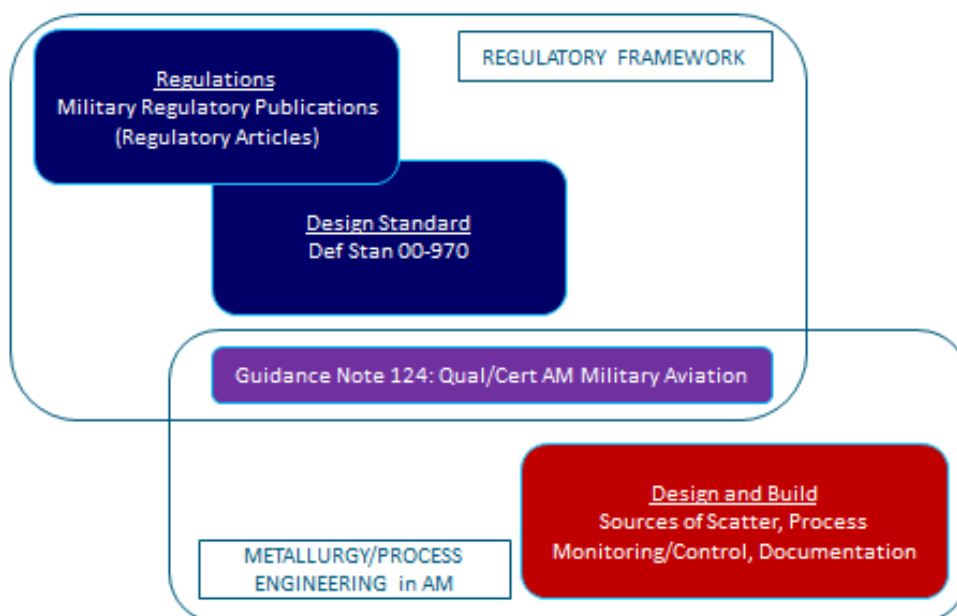


Figure 1: A schematic of how the Guidance Note brings together the existing airworthiness regulatory framework and AM metallurgy / process engineering.

In all 67 recommendations have been made. These are divided into those affecting regulation ('shall'), Acceptable Means of Compliance (AMC) ('should') and Guidance Material (GM) ('may' or 'could'). The background to each recommendation has been explained within the relevant section and the recommendations have been collated into cross-referenced summary tables in the paper.

A summary of the number of recommendations in each category is show in Table 1 below.

Table 1 – Summary of number and types of recommendations for each significant chapter.

Chapter Number / Title	Regulation-Type	AMC-Type	Guidance-Type
3- Airworthiness Assurance of Manufactured Parts (Aircraft Structures)	4	4	1
4 - Airworthiness Assurance of Manufactured Parts (Aircraft Engines)	5	4	4
5 - Part Design and Build	1	40	4

One recommendation from each of the three significant chapters can be highlighted since they represent important discussion points for those working on AM in aviation.

## Chapter 3 - Airworthiness Assurance of Manufactured Parts (Aircraft Structures)

... it is therefore recommended that each Grade A AM part should receive inspection of 100 percent of its surface, and inspection of structurally significant internal areas and areas where defects are likely to occur, using approved non-destructive inspection methods. This wording on non-destructive inspection (NDI) is taken from CS 25.621 Premium Castings and, in the absence of AM-specific guidance, provides a conservative approach to qualification of a part that effectively has no arbitrary scatter factor. Innovations in AM technologies, e.g. in-situ monitoring, could provide alternative means of assuring the defect population of a part without the need for this degree of NDI.

## Chapter 4 - Airworthiness Assurance of Manufactured Parts (Aircraft Engines)

EASA has provided advice, in addition to its regulations, through a Certification Memorandum (CM PIFS-013, Issue 01 The integrity of nickel powder metallurgy rotating critical parts for gas turbines<sup>2</sup>), on the development of a lifing system for powder metallurgy rotating parts, including advice on anomaly characterisation, fatigue testing, probabilistic treatment of inclusions, etc. It is a very important advisory document, which has relevance to AM and it is recommended that it may be used to help those involved in qualification and certification of critical AM aero engine parts to set out an appropriate plan for the establishment of safe cyclic life.

## Chapter 5 - Part Design and Build

For critical AM components a Process Control Document (PCD) shall be supplied as part of the airworthiness documentation. Any changes to the process control document shall be subject to the Military Certification Review Item (MCRI) process. The contents of the Process control document should be written based on the recommendations outlined within this document. The Process control document could include but not be limited to details of the control of:

- AM machine
- Build strategy
- Feedstock
- Post-processing
- Testing

## Conclusions

Any manufacturing method will produce parts that have scatter in their properties, including AM. In fact features of AM mean the sources of scatter are numerous, and in many cases unfamiliar compared to conventional methods, for example because of the use of fine powders as a feedstock material. A crucial theme is that the properties established from coupons, test elements, etc. should accurately represent the scatter in properties, from all sources, in the final part.

---

<sup>2</sup> <https://www.easa.europa.eu/document-library/product-certification-consultations/easa-cm-pifs-013> [accessed 05 March 2019].

## 6 Corrosion management and sensing activities

### 6.1 BEASY Corrosion Manager

*S. Mellings, T. Froome; BEASY*

#### 6.1.1 Service Life Model

By developing an “environmental spectrum” for corrosion caused by galvanic effects when a structure is covered by a film of electrolyte, a Service Life Model has been developed, similar in approach to methodology already used within the aircraft industry for fracture mechanics based structural lifing.

Developments were undertaken with research supported by the ONR Sea Based Aviation Structures & Materials Program.

The new capability was tested on an F/A-18 aileron hinge as shown in Figure 1. The aileron hinge mounts to the rear and aft spars, and to a connecting rib in the outer wing section.

#### Components/Materials

- Aileron Hinge - Aluminium Al-7075
- Large Fasteners x10 (dia. = 0.4 in) - Stainless Steel 17-4PH
- Small Fasteners x7 (dia. = 0.3 in) - Stainless Steel 17-4PH
- Washers - Stainless Steel 17-4PH
- Pin (dia. = 0.675 in) - Carbon Steel S1020
- Bushings (x2) - Al-Bronze AMS 4640

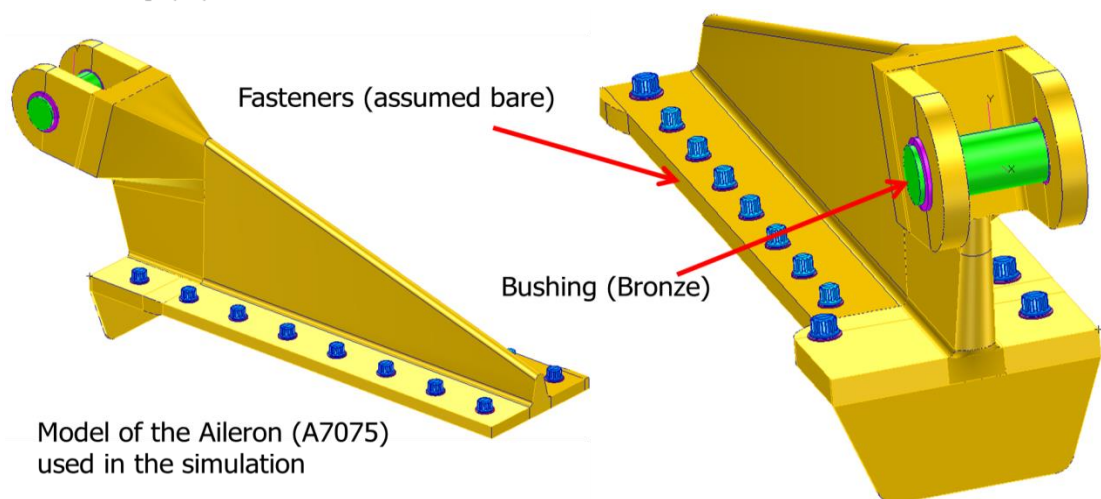


*Figure 1: CAD model of the aileron hinge used in the corrosion Service Life Model simulation*

The model was solved for two representative environmental conditions (different film thickness and conductivity). Corrosion rate and potential are shown in Figure 2.

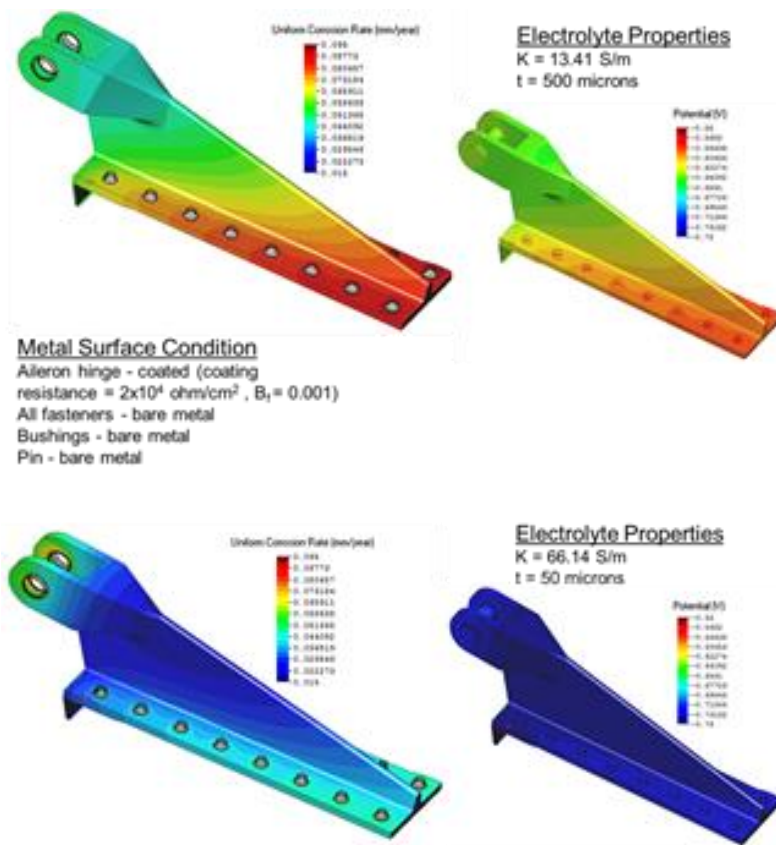


Figure 2: Spatial distribution of corrosion rate and potential

The magnitude and location of peak galvanic stress differs between the two exposure conditions, reflecting the complex interaction between the geometry of the component parts, electrolyte conductivity, film thickness, and the multiple materials (electrokinetics captured through polarization curves). The peak galvanic stress occurs around the remote (i.e. away from the hinge end) fasteners under the WET exposure condition and at the bushing-lug interface for the SEMI-WET exposure condition.

Cumulative corrosion damage could then be predicted using the corrosion rates determined from each of the defined exposure conditions in combination with an environmental exposure spectrum, and is shown in Figure 3. The model matched the location of the corrosion damage observed from tear down (as highlighted), with high corrosion rates near the bushing and more remote fasteners.

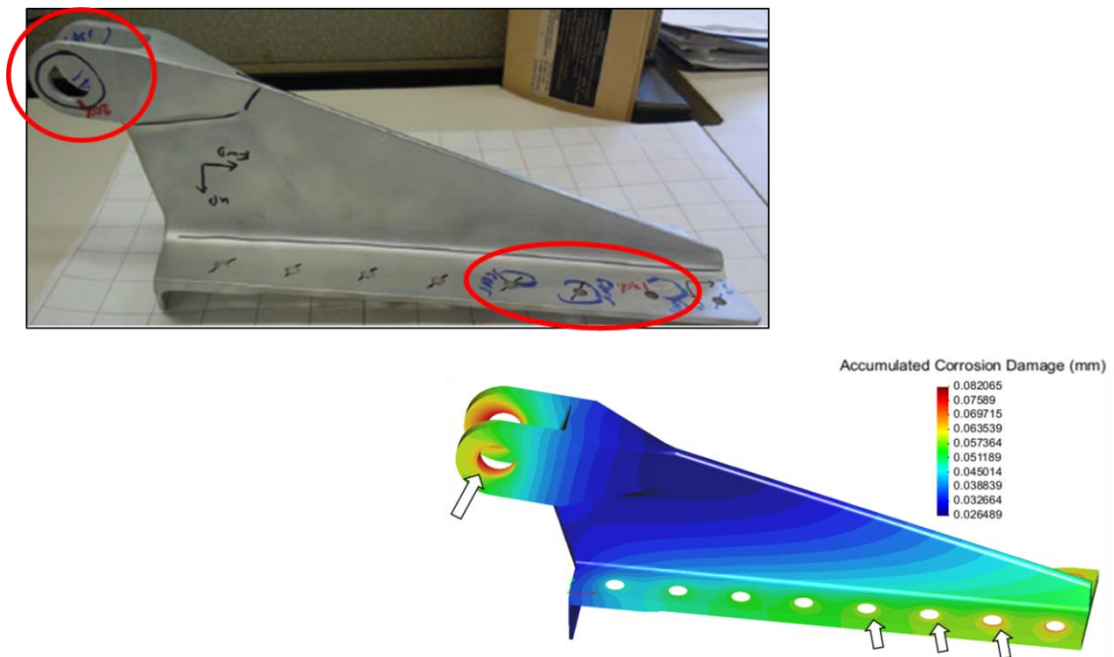


Figure 3: Comparison of accumulated corrosion damage

### 6.1.2 Corrosion through surface finish and of Crevices

Additional development has made available the capability for simulation of spatial and temporal (time dependent) behaviour, caused by corrosion of a surface finish or sacrificial coating and which then results in exposure of the underlying substrate.

A test specimen evaluated consisted of two plates (Super duplex (SD); Aluminium) clamped together by SD nuts and bolts with Aluminium washers in contact with the SD plate.

Images in Fig 4 show the differences in corrosion rate behaviour between a scenario with a crevice (100 micron wide at the opening between plates) and a scenario with no crevice.

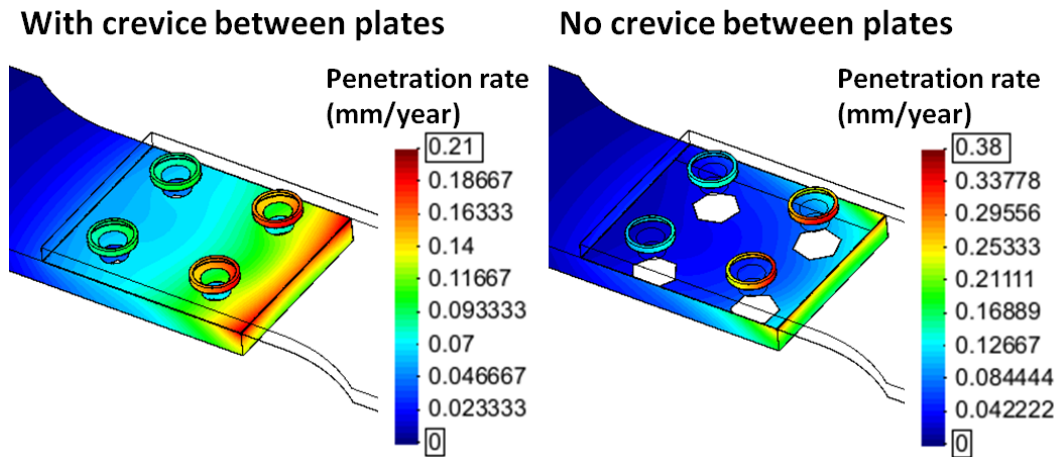


Figure 4: Comparison between Crevice and No Crevice scenarios

A separate transient simulation was then undertaken to identify behaviour at various intervals, with Fig 5 providing two snapshots before and after a time when corrosion had consumed a Cd plating on the super duplex material, resulting in further observable modification to the behaviour (distribution and rate).

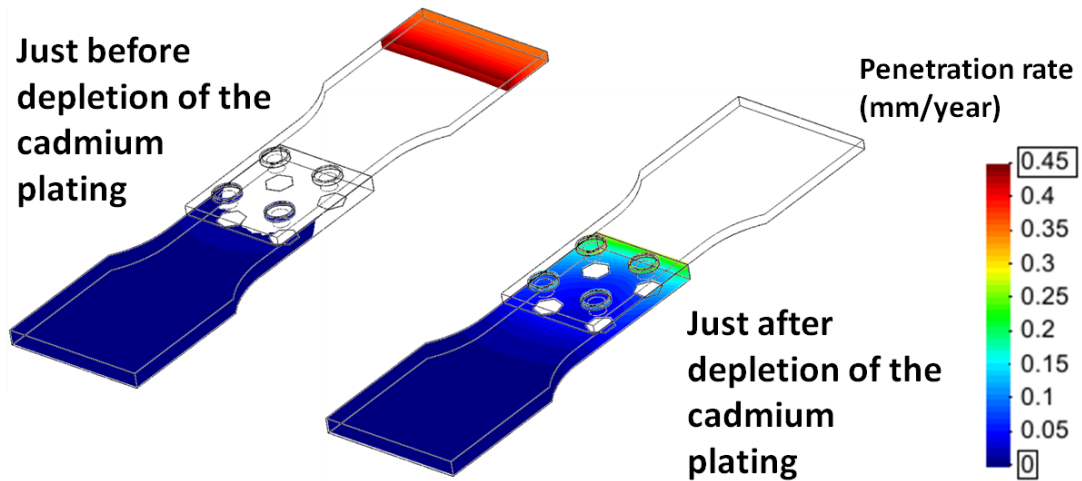


Figure 5: Behaviour before and after the point at which Cd plating became fully consumed

Progression from this development will lead towards determination of modified surface morphology, and identification of severity of associated stress concentrations.

## 6.2 Development of a structural repair and corrosion database for UK military aircraft

*M. Hodge, A. Parrish, Musketeer Solutions*

After the Aloha Flight 243 explosive decompression in 1988, awareness was raised of the risk of structural failure caused by coincident airframe repairs accumulated over time. Following this incident, operators of pressurised aircraft, in particular, were required to maintain accurate structural configuration control supported by detailed records of structural damage and repairs along with their precise locations and requirements for Repair Assessment Programmes were mandated by the regulators. Research by Musketeer Solutions, on behalf of the UK Defence Science and Technology Laboratory, has developed a set of databases, with easy to use, graphical user-interfaces that provide a scalable solution to this requirement. Musketeer Solutions' research has been undertaken predominantly in the Military environment but covers many aircraft types from large and medium civil-derived passenger aircraft to helicopters. Even the Royal Air Force's GRP gliders have been surveyed as part of the process of establishing an intuitive, easy to populate and easy to access database of corrosion and damage repairs. The military context is perhaps the most difficult to assess for a number of reasons, some of which stem from initial procurement when civil aircraft, often pre-used, are converted to military use without a full record of corrosion or structural repair. When one factors-in the need to regularly modify military aircraft throughout their life, the often-hostile environment in which they are flown and the austere environment in which they are sometimes maintained, the importance of an accurate record of structural issues becomes even more important. The lengthy service life of military aircraft, and the desire to extend that life to ensure value for the taxpayer, all support the case for a consolidated, accurate database of damage and corrosion. Indeed, the UK Military Airworthiness Authority mandates the collection of such information in its Regulatory Article on Structural Integrity Management (RA 5720) and recommends that 'Ideally, a single database should be used to maintain Structural Configuration Control.'

It is with this in mind that Musketeer Solutions developed a Structural Repair and Corrosion Database (StRaCD), tailored to each aircraft type and with the emphasis on a visual approach (Figure 1). Diagrams are clear and can be easily expanded to show more detail without loss of positional accuracy of each repair. As well as satisfying the requirements of the regulator, StRaCD meets the user need for centralised access to repair data that can be exploited in support of Structural configuration Control.

StRaCD provides reports by several filters (Figure 2) including date-range, major structural component, location and can even relocate repairs to cannibalised structural components. Trending of repair arisings can be easily achieved and the database can be used to inform the re-lifing of repairs as well as support pre-input maintenance surveys.

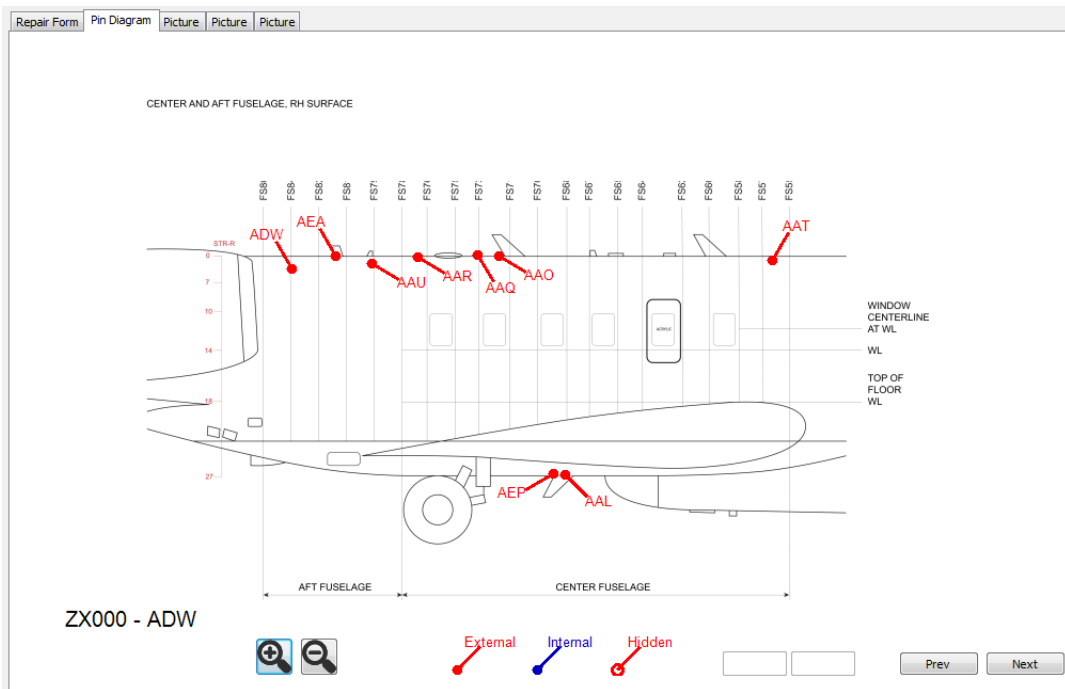


Figure 1: 2-D Projection of Aircraft with Recognised Location Information and the ability to zoom in and out, scroll around aircraft and navigate between illustrations

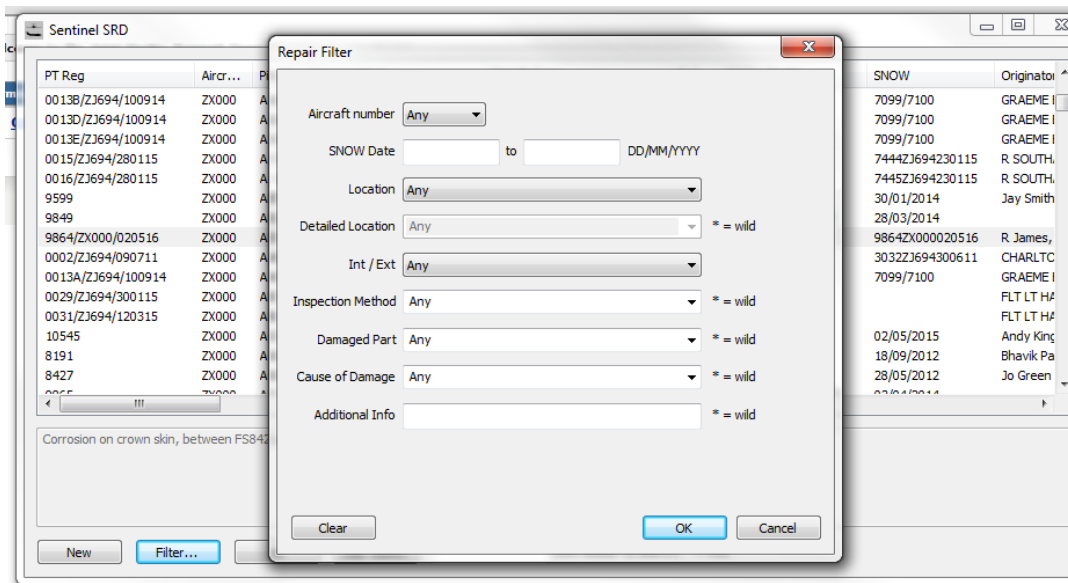


Figure 2: Flexible filter and export functions to allow efficient exploitation

However, initial usage of StRaCD has produced some issues to consider, for whilst StRaCD is a good management tool, it does rely on accurate and complete population of repairs and corrosion. For new aircraft fresh off the production line this should not pose a problem but for legacy fleets accurate data capture is vital. Where original repair data is unavailable StRaCD allows decision makers to record that a

repair of unknown provenance exists. As well as completeness, the location and format of existing repair records can also present a challenge when populating the database as conversion from legacy format must be undertaken. Finally, secure access to such sensitive information must be considered to guard against malicious exploitation or, more likely, corruption of the data by the uninitiated. To counter this latter point StRaCD requires engineering expertise to populate and exploit but makes maximum use of drop-down menus with free-text reduced to the minimum necessary (Figure 3).

The screenshot displays a web-based repair form with the following sections:

- 2 - DAMAGE TYPE / MEASUREMENT (use appropriate tools, ie. depth guage, mylar etc.)**
  - Damage Type: Corrosion
  - If 'Other', please specify: Surface
  - If Corrosion: Other (please specify)
  - If Corrosion Uniform:  Light  Medium  Heavy
  - PSE/SST Affected: No
  - If Corrosion:  Widespread  Localised
- 3 - DAMAGE TO UNDERLYING STRUCTURE (Frame, Stringer, Rib, etc.)**
  - Yes  No  Unknown (not accessed)
  - If 'Yes', please enter details here:
  - SRPSA (if applicable): Aircraft ZX000
- 4 - OTHER REPAIRS / MODIFICATIONS IN THE AREA**
  - Yes  No  Unknown (not accessed)
  - If 'Yes', please enter details here, including edge to edge distance from adjacent repairs
- 5 - ADDITIONAL INFORMATION (use sketches, rubbings or diagrams as necessary)**
  - Additional documents, pictures or sketches: 3 Artefacts
  - Type as required, there are no space limitations.
  - Corrosion on crown skin, between F5842 and F5845, 18"-23" RHS of CL. Six fasteners affected.

Figure 3: Example screenshot of repair form.

StRaCD exploits COTS technology and has proved to be a cost-effective tool in support of Structural Integrity management. Constructed using modules and concepts that are easily transferrable it is flexible and can be tailored to suit individual platforms. Already utilised by a number of UK Military aircraft types it has been extremely well-received by their engineering communities.

6.3 Corrosion Sensor Development, Characterisation & Deployment

A. Cafearo, R. Eley, C. Figgures, I. Sturland and M. Balmond, BAE SYSTEMS Advanced Technology Centre

The cost of corrosion to the aerospace industry is considerable. In 2018, the US Department of Defence (DoD) reported a cost of 37 billion dollars in the US alone and 12 billion of this cost was related specifically to the aerospace sector. More than 2/3 of the annual cost of corrosion faced by the US DoD is actually considered preventable and so BAE Systems have developed corrosion sensing technology in order to actively monitor the situation within the internal bays of aircraft. Internal bays have been targeted because they are traditionally expensive and difficult to visually inspect.

Key points:

- The sensors provide a cost saving by deferring the cost of inspections when there has not been any corrosive activity within a bay.
- The sensors are far more sensitive than visual inspections which means that corrosion can be detected early and can be dealt with by pro-active maintenance before the issue becomes a more serious and costly problem.
- The sensors are coated with the same paint scheme as the aircraft and act as “smart witness plates” monitoring the degradation of the paint coating as a result of the environment within the bay (figure 1).
- Sensors can be located in areas that are difficult to access (within sealed bays, behind equipment etc.)

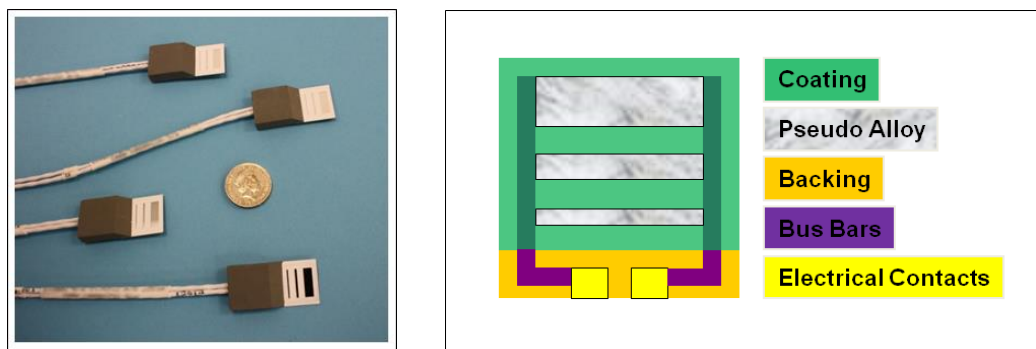


Figure 1: Image of corrosion sensors & schematic of 3-slot sensor configuration

Aircraft primers contain inhibitors which can protect structure that becomes exposed due to any “defects” in the coating (e.g. scratches). The protection continues until the inhibitors eventually become depleted and then, at this point, the underlying aluminium alloy will begin to corrode. The inhibitors can protect the alloy longer when the defects in the coating are smaller and so the sensor uses different slot widths in

order to monitor the rate of paint coating depletion with respect to coating defects of different sizes.

If fitting to aircraft that have strain-gauge health monitoring on-board, the corrosion sensors can be connected into the same type of port that the strain gauges use and the outputs can be monitored through the existing system. This enables data to be collected from all aircraft and assessed on a fleet-wide basis to enable maintenance planning.

If retro-fitting to aircraft that do not already have an existing health monitoring system on-board then this just means that a data logger has to be installed on the aircraft along with the sensors. There are various options available for collection of data from the loggers (with varying degrees of automation) and the particular method to be employed can be determined based on the customer's requirements and operating procedures.

Aim: Monitor 24/7, catch corrosion early before it becomes a serious problem and enable planning of inspections/maintenance to be carried out long in advance by means of continuous condition monitoring.

### 6.3.1 Developments to date

- Sensor operation has been proved by outdoor characterisation testing and accelerated testing in the lab.
- Sensors have been developed with both 2000 & 7000 series sensing elements and with both chrome & chrome free primer coatings.
- Sensors have been tested in conditions covering four orders of magnitude of corrosion severity, from standard salt spray though to fairly benign cyclic humidity testing.
- A novel sensor packaging production technique has been developed which enables the manufacture of units that are robust enough for long term use in harsh environments
- Sensors manufactured using the new packaging process have survived long term immersion testing in salt solution, thermal shock testing and reliability/durability testing (vibration testing, combined temperature humidity testing and temperature cycling over the full mil spec temperature range). The process has also been productionised in order that it is suitable for volume manufacture.
- Sensors are currently fitted to every F-35 aircraft that is produced and the outputs from all sensors are monitored remotely through the on-board Autonomic Logistics Information System.
- Trials have been carried out on Typhoon, Tornado, Hawk, Sentry, various Ships & Land Vehicles with a view to developing sensor variants & data logging systems appropriate for use with sensors when retro-fitted to platforms that do not have existing ports available for the connection of corrosion sensors.

## 6.3.2 Summary

- The PCD sensor can monitor paint coating degradation 24/7 and can provide an early warning of corrosion.
- Areas that are difficult to access can be monitored without the need to open up the bay/compartment to carry out inspections.
- The sensors are very sensitive and provide alerts when corrosion pits begin to form that are only 30 microns in diameter (far earlier than they can be seen by the human eye). Knowing about corrosion events this early means that the issue can be dealt with before it becomes serious.
- One of the biggest costs of corrosion is the cost of inspections. By using sensors to monitor continuously and avoiding the need to access all locations on such a frequent basis, big savings can be made on inspection costs.
- The PCD sensor can monitor paint coating degradation 24/7 and can provide an early warning of corrosion.
- Areas that are difficult to access can be monitored without the need to open up the bay/compartment to carry out inspections.
- The sensors are very sensitive and provide alerts when corrosion pits begin to form that are only 30 microns in diameter (far earlier than they can be seen by the human eye). Knowing about corrosion events this early means that the issue can be dealt with before it becomes serious.
- One of the biggest costs of corrosion is the cost of inspections. By using sensors to monitor continuously and avoiding the need to access all locations on such a frequent basis, big savings can be made on inspection costs.

## 7 Developments in fatigue analysis and fracture assessment tools

### 7.1 Developments in fatigue analysis - HBM Prenscia

*A. Halfpenny and R. Plaskitt, HBM Prenscia*

#### 7.1.1 General Developments

HBM Prenscia continue to develop their material fatigue testing capabilities and the fatigue damage models used in their nCode software products for fatigue and durability analysis.

- nCode DesignLife, for fatigue analysis from finite element analysis stress results, has been developed to support a unified strain-life fatigue and fracture mechanics crack growth model. This uses the finite element analysis stress at a node, the stress distribution along the crack path, and optionally any residual stress distribution along the crack path.

This “Total-Life” model is based on the work of Glinka and Mikheevskiy [1], and an extended abstract is included in this review to describe the model.

- nCode Aqira has been developed for probabilistic fatigue and reliability simulation, combining DesignLife deterministic fatigue analyses with ReliaSoft stochastic analyses. This uses a ‘Monte Carlo’ design of experiments approach combined with ‘Latin Hypercube’ sampling to simulate reliability tests based on existing finite element analysis models to quantify robustness.

This probabilistic approach is described in an extended abstract included in this review.

- The Advanced Materials Characterisation & Test laboratory (AMCT) has completed strain-controlled fatigue tests on additively manufactured titanium Ti-6Al-4V alloy, manufactured by electron beam powder bed fusion (E-PBF), with and without post manufacture HIP treatment, and in vertical, horizontal and 45-degree build layer orientations.

This work will be presented at ICAF 2019 and the abstract is included in this review.

#### 7.1.2 The “Total-Life” model - an Analysis Method for Combining Crack Initiation and Crack Growth Models in Structures

Fatigue cracks initiate and grow as part of a two-stage process; Stage 1 - crack initiation, and Stage 2 - crack growth. Historically fatigue analyses of these stages have been addressed using separate physical models. Crack initiation has typically used a strain-life (EN) damage model, and crack growth has used either a Linear Elastic Fracture Mechanics (LEFM) or an Elastic-Plastic Fracture Mechanics (EPFM) model.

The classical stress-life (SN) damage model does not distinguish between these two fatigue processes. It effectively combines both processes into a single ‘total-life’

curve. However, in the case of traditional test specimen geometry, stage 2 crack growth occurs rapidly when compared with the stage 1 initiation life, so an SN curve is typically assumed to represent the initiation life of the material.

The Total-Life model combines aspects of both the strain-life (EN) and fracture mechanics (LEFM) models into a unified model for fatigue life estimation. This model can produce fatigue life estimates that are considerably more accurate than the classical approaches.

This is particularly apparent with thick welded structures, cast structures, and for aerospace applications, in lightweight structures, such as lightweight aluminium panels with riveted joints. In these cases, a significant period of time is spent in both initiating and propagating the crack to failure.

In many cases a crack will propagate into a low-stressed region and this can result in the crack arresting and never propagating to failure. In these cases, it is important to recognise that these cracks do not compromise the durability of the structure and may be acceptable in-service.

Consider a fatigue crack growing through an infinite flat plate as illustrated in Figure 1. This figure illustrates an idealised grain structure where each grain has a radius approximately  $\rho^*$  ("rho star"). The opening and closing action of the crack creates persistent slip bands in the grains immediately ahead of the crack tip. These give rise to local stage 1 fatigue damage within the grain. This grain becomes progressively weaker with each cycle until it fails and the crack advances.

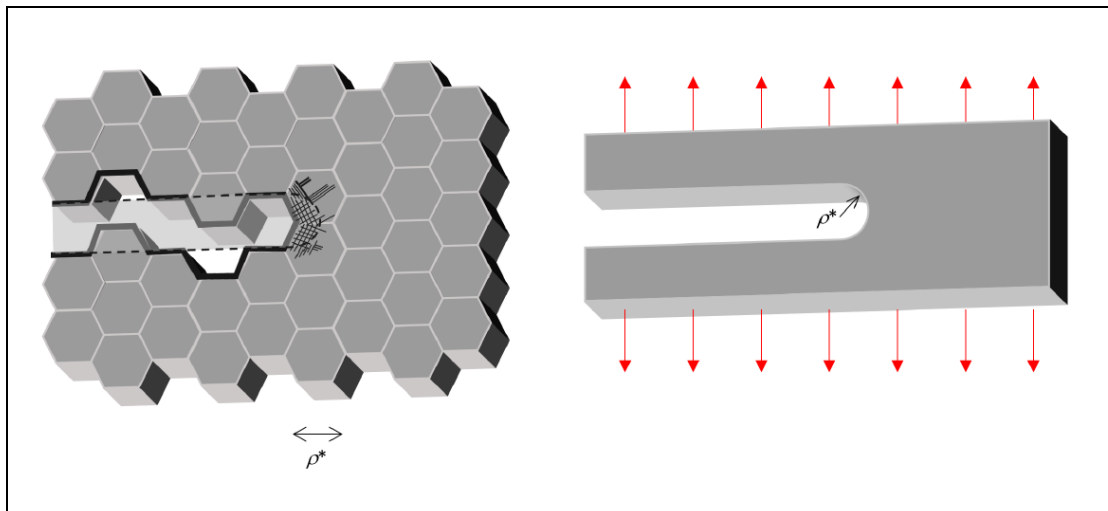


Figure 1: Idealisation of a crack growing through an infinite plate

This Total-Life model is based on the work of Glinka and Mikheevskiy [1]. Glinka's original hypothesis considers the local failure of each idealised grain as equivalent to a local crack initiation failure. The progressive crack growth is therefore seen as a sequence of successive initiation failures. As the crack becomes longer the stress intensity will increase giving rise to an increase in strain energy and the failure of each grain will occur more rapidly until fast fracture occurs. Glinka was able to correlate this hypothesis with measured fatigue cracks giving rise to a 'unified fatigue/fracture' model; one that is able to accurately determine the total-life of a

fatigue failure inclusive of both stage 1 crack initiation and the subsequent stage 2 crack propagation.

This Glinka model is similar to the Linear Elastic Fracture Mechanics (LEFM) model, but whereas LEFM assumes an infinitely sharp crack, Glinka assumes a blunt crack of tip radius  $\rho^*$ . Where  $\rho^*$  is a material fitting parameter of similar size to the grain size of the material. This assumption avoids the stress singularity that is associated with LEFM, and this permits the use of a non-linear elastic-plastic stress distribution ahead of the crack.

The unification of stage 1 and 2 damage models also allows parameters for crack growth to be estimated from strain-controlled (EN) fatigue tests, and visa versa. However, for greater accuracy it is normal practice to use both strain-life and crack growth tests to derive the properties.

The calculation of parameter  $\rho^*$  is essential to this Total-Life model. Mikheevskiy [1] suggests 3 approaches to estimating this parameter:

1. Estimate based on the fatigue limit and the threshold stress intensity range.
2. Estimate based on experimental fatigue crack growth data at various stress ratios.
3. Estimate based on the strain-life (EN) curve and limited fatigue crack growth data.

This Total-Life model including parameter  $\rho^*$  estimation, and a case study for thick plate welded structures, will be presented at SAE World Congress 2019 [2] and [3], and NAFEMS World Congress 2019 [4]

### References

It is intended to submit this work to ICAF 2021, to include a case study for lightweight aluminium panels with riveted joints for aerospace applications.

[1] Mikheevskiy, S., 2009, "Elastic-Plastic Fatigue Crack Growth Analysis Under Variable Amplitude Loading Spectra," PhD thesis, University of Waterloo.

[2] Munson, K., Mentley, J., Halfpenny, A., 2019 "A finite element based methodology for combined crack initiation and crack growth prediction in welded structures", SAE Technical Paper 2019-01-0537, SAE World Congress, April 9-11, 2019, Detroit

[3] Cordes, T., Norton, E., Brown, H., Munson, K., 2019 "Comparison of Total Fatigue Life Predictions of Welded and Machined A36 Steel T-Joints", SAE Technical Paper 2019-01-0527, SAE World Congress, April 9-11, 2019, Detroit

[4] Halfpenny, A., Munson, K., Mentley, S., Roberts, P., 2019 "Fatigue Simulation of Welds using the Total-Life Method", Technical Paper NWC19-295, NAFEMS World Congress, June 17-20, 2019, Quebec City, Canada

7.1.3 Probabilistic Fatigue and Reliability Simulation

The fatigue design of mechanical systems has historically followed a ‘deterministic’ process. That means, for a given set of inputs they will return a consistent set of fatigue life results with no scatter. In reality the inputs are statistically uncertain – they have an expected value and a variability. Deterministic design methods take no implicit account of uncertainty. In practice, the designer applies a safety factor to each input parameter to account for the uncertainty. Often an additional safety factor is also applied to the final result to allow for ‘modelling errors’. In most cases, the engineer is fairly certain that the simulation results are conservative, but cannot state with any confidence what the expected safety margin, reliability or failure rate will be.

In comparison, a ‘Probabilistic Fatigue Simulation’ is ‘stochastic’ in nature. This means inputs are expressed using an expected value along with a probability distribution. The analysis is run repeatedly using a procedure known as ‘Monte Carlo’ simulation. A different set of input values is chosen randomly for each run based on the specified statistical distributions.

This produces a number of life results. Post processing of these results provides a safe design where the reliability statistic can be determined with known confidence. This design process helps to avoid poor in-service reliability whilst reducing over-design. Furthermore, it is easy to see which uncertainties contribute most to the overall design conservatism allowing justification to study these uncertainties more thoroughly.

A comparison between deterministic and stochastic design methods is illustrated in Figure 2.

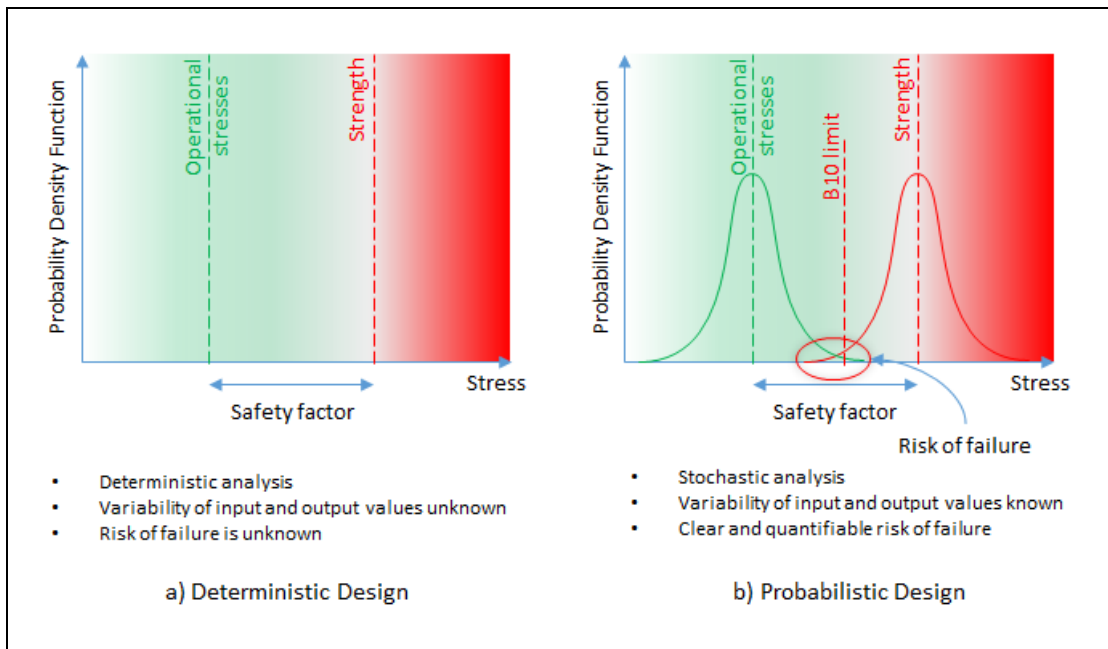


Figure 2: Comparison between deterministic and stochastic methods

Traditional fatigue analyses are performed through a deterministic calculation process where input parameters are assigned constant values. The same process can be implemented stochastically by embedding the deterministic process inside a

'Monte Carlo wrapper' as illustrated in Figure 3. The 'wrapper' runs the deterministic process repeatedly. The input parameters are varied statistically with every run. The variations follow user-defined probability distributions. This creates a sample of simulated fatigue life results which are post-processed using reliability analysis methods to quantify reliability and robustness.

The stochastic simulation method used is based on the 'Monte Carlo' method using 'Latin Hypercube Sampling'. The 'Monte Carlo' with 'Latin Hypercube' sampling technique is used to determine the reliability of a design, whilst 'Factorial Sampling' and 'Response Surface' techniques are used to determine the robustness of a design.

A robust design considers permutations of the stochastic input parameters that lead to the most extreme responses. These combinations may have a low likelihood of occurring, however they will result in the worst case conditions. Simulation is required to determine whether the component will survive these conditions, or whether their probability of occurrence is acceptably low.

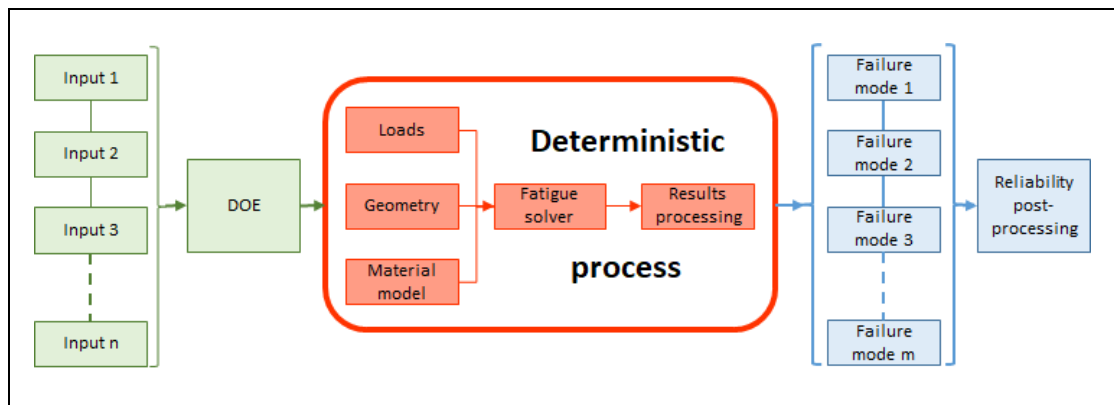


Figure 3: Schematic of a probabilistic design analysis

This probabilistic fatigue and reliability simulation, and a case study analysis of an air-cooled intercooler manufactured from pressed sheet aluminium, will be presented at NAFEMS World Congress 2019 [1].

## References

- [1] Halfpenny, A., Chabod, A., Roberts, P., Bonato, M., 2019 "Probabilistic Fatigue and Reliability Simulation", Technical Paper NWC19-294, NAFEMS World Congress, June 17-20, 2019, Quebec City, Canada

**7.1.4 Strain-controlled fatigue testing of additive layer manufactured titanium alloy Ti-6Al-4V**

Additive-layer manufacturing (ALM) methods are developing rapidly in many industries to reduce weight and lead times; with an additional advantage in aerospace for significant reduction in material buy-to-fly ratio. Aerospace OEMs and suppliers are identifying appropriate applications for ALM components and progressing their use from development prototypes, into components qualified for service on production aircraft.

This paper describes strain-controlled fatigue testing of a titanium Ti-6Al-4V alloy, additive layer manufactured by two powder bed fusion methods; electron beam melting (EBM) and selective laser melting (SLM).

The EBM additively manufactured material includes comparison of results from material with no post-manufacture heat treatment (“as-built”) and after a hot isostatic pressing (HIP) treatment. This HIP treatment condition is further examined to assess directional fatigue properties, using specimens manufactured with build directions vertical, horizontal and at 45 degrees to the axis of the specimen.

These fatigue test results are compared with those for similar titanium Ti-6Al-4V alloy manufactured by traditional wrought mill and by powder metallurgy hot-isostatic pressing.

An example comparison for EBM in the as-built and HIP conditions, both with vertical build direction, compared with wrought mill stock, is shown in Figure 4.

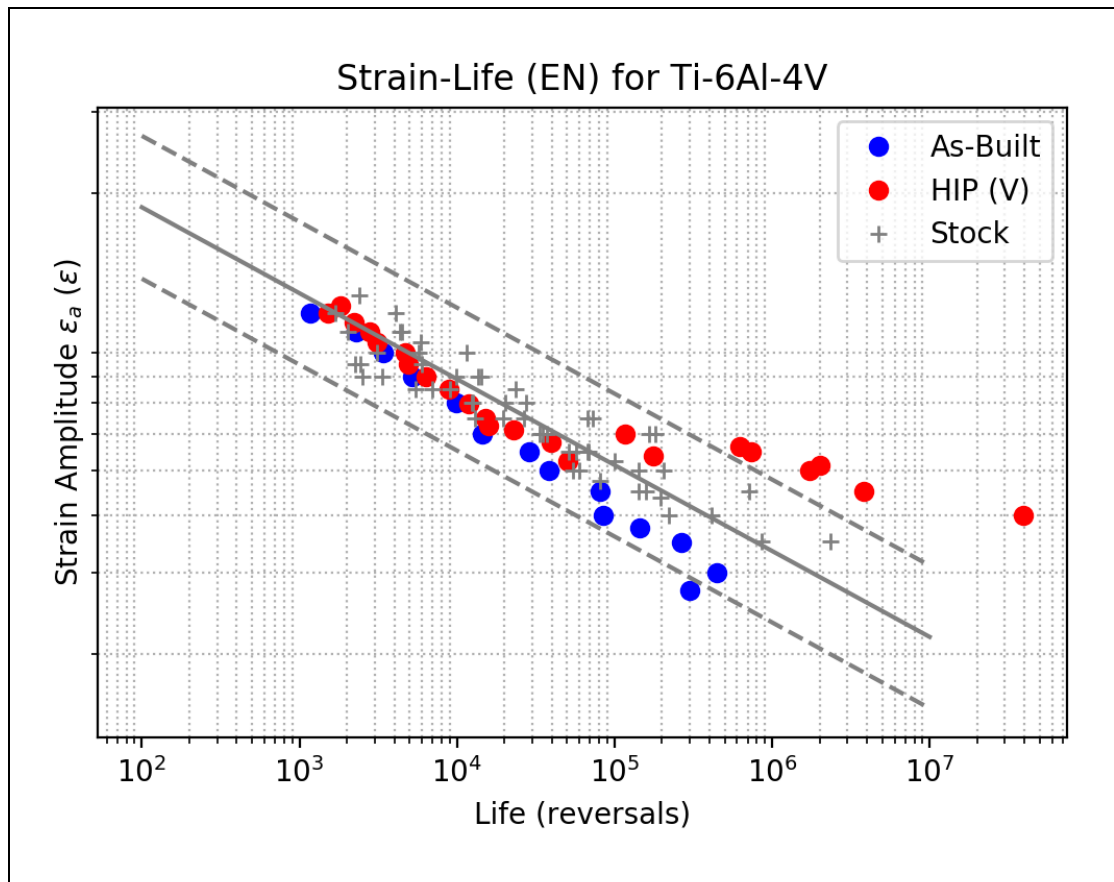


Figure 4: Comparison of fatigue test results for EBM, as-built and HIP conditions, with wrought stock.

## 7.2 BEASY Fracture Assessment Tool (FASST)

*S. Mellings, T. Froome; BEASY*

This new capability has been introduced to provide fast and effective evaluation of the effect of a crack on structural integrity and allows account to be taken of load redistribution and geometric effects (ie where it is appropriate to need to go beyond conventional Handbook approaches).

Parts of the model where cracks may be critical can be readily conceptualised, providing identification, for example, of sensitivity to manufacturing defects (treated in worst cases as cracks) without the need to identify a "nearest" or "best" handbook solution for the target location.

Excel macros can be used to automate creation of graphs, showing (for example):

- SIF values for defined crack sizes
- The applied load required to generate a target SIF value
- The change of SIF along a line of points in a structure

Creating a plot of SIF versus crack size (for a crack at a selected location) allows easy identification of the size at which SIF would become critical and the part could be expected to fail.

Alternatively, creating a plot of applied load versus SIF (for a crack of a particular size at a selected location) allows easy identification of the load at which SIF would become critical and the part could be expected to fail.

Results can be created:

- Using "reference solutions" to determine SIF values: standard handbook solutions are applied together with stresses taken from the BEASY model of the un-cracked structure.
- Using "BEASY simulation" to determine SIF values by solving a series of models, each of which includes one crack. This provides an accurate calculation of the SIF values, taking into account load redistribution and geometric effects (aspects that are not incorporated in the "reference solutions").

Assessment can be made with single or multiple load cases. SIF results of multiple load cases can be combined in various ways.

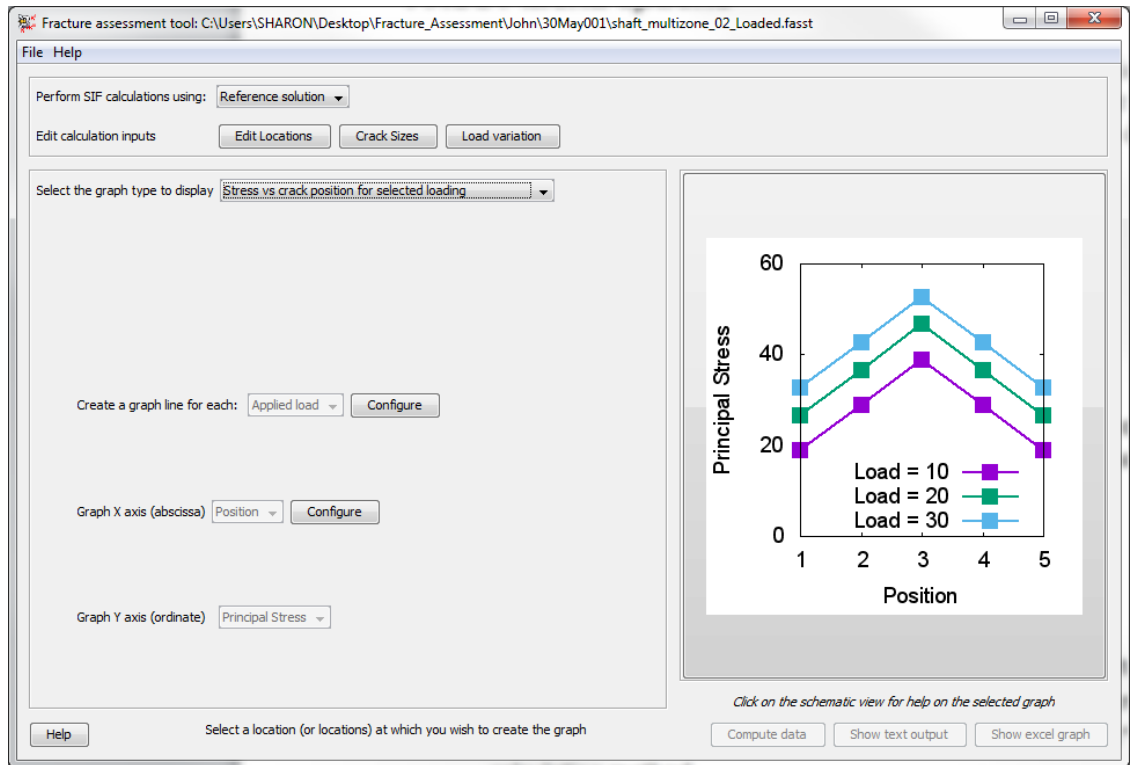


Figure 1: Example view of the FASST main panel

## 7.3 A Framework to Implement Probabilistic Fatigue Design of Safe-Life Components

*J. Hoole<sup>1</sup>, P. Sartor<sup>1</sup>, J. Booker<sup>2</sup>, J. Cooper<sup>1</sup>, X.V. Gogouvitis<sup>3</sup>, A. Ghoul<sup>4</sup>, R. K. Schmidt<sup>5</sup>*

<sup>1</sup>*Department of Aerospace Engineering, University of Bristol, United Kingdom*

<sup>2</sup>*Department of Mechanical Engineering, University of Bristol, United Kingdom*

<sup>3</sup>*Safran Landing Systems, Gloucester, United Kingdom*

<sup>4</sup>*Safran Landing Systems, Vélizy, France*

<sup>5</sup>*Safran Landing Systems, Ajax, Ontario, Canada*

This entry is an abstract. The full paper can be found in the ICAF2019 proceedings.

Within the aerospace sector, aircraft landing gear are classified as ‘safe-life’ components [1]. The ‘safe-life’ of a component represents the life (often defined in flight-hours or flight-cycles) at which the component must be retired from service. Component safe-life values are computed using ‘classical’ fatigue analysis methods, such as a stress-life approach incorporating Miner’s Rule [1]. However, safe-life fatigue analysis contains many sources of variability within the design parameters of the analysis process, such as scatter in material properties and uncertainty in loading. This variability propagates through the analysis process into component safe-life values and is currently accounted for using conservatism and safety factors. The use of safety factors is known as a deterministic mindset or approach, whereby all design parameters are set to single and safe values. The introduction of conservatism into the analysis process could lead to components being ‘over-sized’, increasing component weight and life-cycle cost, thereby compromising the performance of the overall structure [2]. In addition, conservatism can also lead to the potential component safe-life not being fully exploited due to early retirement from service.

Probabilistic approaches to fatigue design and analysis enable the variability in design parameters to be statistically characterised using probability distributions (e.g. Normal, Weibull, etc.) [3]. The statistical characterisation of design parameters permits the variability to be propagated through to the output of the safe-life analysis process to produce a probability distribution of the accumulated fatigue damage or the component safe-life. The component reliability (or probability of failure) associated with the component safe-life can then be computed from the output probability distribution. As a result, probabilistic approaches enable a more accurate representation of the statistical nature of fatigue design parameters and have been successfully applied to the fatigue analysis of safe-life components in the Light Aircraft [3] and Rotorcraft sectors [4]. A probabilistic approach offers the opportunity to better represent and understand the variability within component safe-life values, increasing the confidence in the component retaining its structural integrity throughout its design life. This increased confidence has the potential to yield more efficient designs that remain safe in-service.

Current research work by the authors aims to develop a probabilistic approach for the fatigue design and analysis of safe-life aircraft landing gear components. This paper

aims to document the authors' experience in the development of a probabilistic approach to date, as well as identifying on-going challenges and considerations for future implementation. This will be achieved by briefly introducing the methods required to support a probabilistic approach, along with discussing the 'mindset' that engineers will need to adopt to ensure the successful implementation of a probabilistic approach in the future.

Whilst probabilistic approaches offer opportunities to reduce the conservatism currently required in fatigue design, the additional technical knowledge that must be developed is significant. To capture the authors' experience in attaining this technical knowledge, this paper will provide an entry-level introduction into the core method types required for a probabilistic approach and the challenges of selecting such methods:

- Statistical Characterisation: *the selection and fitting of probability distributions to design data.*
- Probabilistic Fatigue Method: *the propagation of variability.*
- Surrogate Modelling: *the approximation of computationally-demanding processes.*
- Sensitivity Analysis: *the use of probabilistic results to identify design drivers.*

Beyond the additional implementation of new methods, the adoption of a probabilistic approach will also require practising engineers to adapt to a new mindset of accepting variability in design parameters and component safe-life values, compared to the deterministic mindset currently used. The paper will present how systematic processes can be used to increase the understanding and confidence in results from the statistical characterisation of design data, to support the transition to the probabilistic mindset. In addition, the change of mindset will also require the development of probabilistic design criteria, in the form of 'target reliabilities' and potential routes to defining such criteria will also be discussed.

The reluctance to employ probabilistic approaches is also often founded in the additional effort and resources required, compared to a deterministic approach, in terms of required data, computational resources and time to develop and learn methods [5]. Therefore, this paper will conclude by demonstrating how the methods required for the probabilistic design and analysis of safe-life components can support other design activities and developments in the aerospace sector, to increase the potential utility of probabilistic methods. As aerospace fatigue design is entering the age of 'big-data' [6], systematic and robust statistical characterisation methods are required to fully exploit the data being generated, especially from the in-service monitoring of aircraft. In addition, as optimisation becomes ever more deployed within aerospace structural design, the need for faster evaluations of finite-element programs can be supported through surrogate modelling. Likewise, the introduction of 'digital twins', whereby an often computationally expensive mathematical model of the in-service component is updated based upon in-service data in real-time [6], is likely to require surrogate modelling methods.

In summary, the development of a probabilistic approach would not only permit reduced conservatism within the fatigue design and analysis of safe-life components

but will also support other rapidly developing areas of aerospace fatigue design. Figure 1 summarises the paper, providing an overview of how the different methods of a probabilistic approach can be combined to support the development of more efficient and optimised components. This paper presents work performed as part of the Aerospace Technology Institute funded “Large Landing Gear of the Future” project in collaboration with Safran Landing Systems.

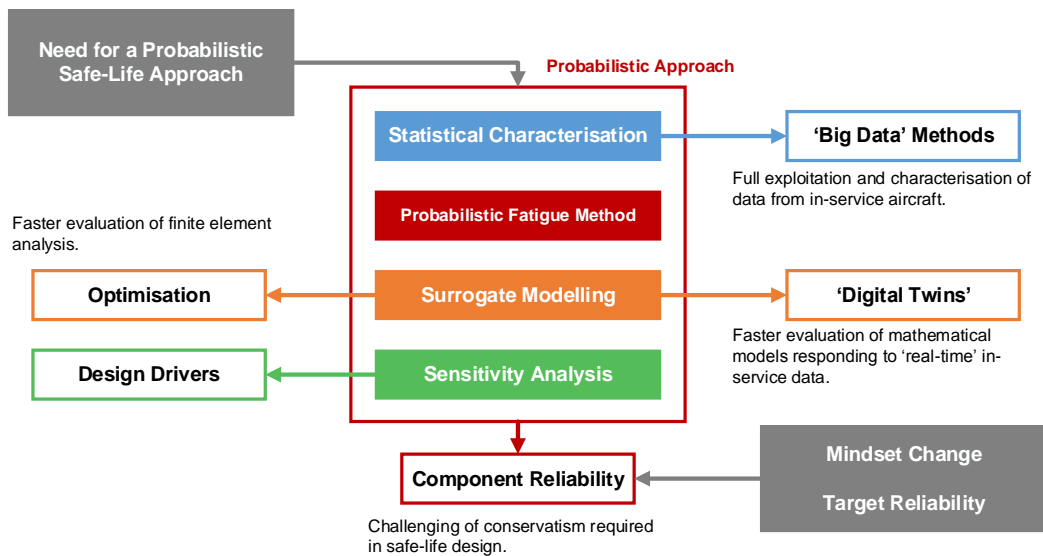


Figure 1: An overview of the methods required for performing probabilistic fatigue analysis and how they can be used to support other advances in aerospace fatigue design and analysis.

**References**

- [1] Braga, D. F. O., et al. *Advanced design for lightweight structures: Review and prospects*, Progress in Aerospace Sciences, **69**, 2014, 29-39.
- [2] Suresh, S. *Fatigue of Materials*, 2<sup>nd</sup> Edition, Cambridge University Press, 1998.
- [3] Ocampo, J, et al. *Development of a Probabilistic Linear Damage Methodology for Small Aircraft*, Journal of Aircraft, **48** (6), 2011, 2090-2016.
- [4] Zhao, J., Adams, D. O., *Achieving Six-Nine’s Reliability Using an Advanced Fatigue Reliability Assessment Model*, Proceedings of the American Helicopter Society 66<sup>th</sup> Annual Forum, 2010.
- [5] Goh, Y. M., et al. *Improved utility and application of probabilistic methods for reliable mechanical design*, Proceedings of the Institution of Mechanical Engineers, Part O: Journal of Risk and Reliability. **223** (3), 199-214.
- [6] Graham, K., et al. *Aircraft Fatigue Analysis in the Digital Age*, Proceedings of the 29<sup>th</sup> Symposium of the International Committee on Aeronautical Fatigue and Structural Integrity (ICAF2017), 2017.

## 7.4 Rapid Calculation of Safe Acceleration Values for Aircraft Structures under Flight Test

*S. S Dosman<sup>1</sup> and J. Gorman<sup>2</sup>*

<sup>1</sup>*AV8R Consulting, Cambridge, UK; email:*

<sup>2</sup>*Marshall Aerospace & Defence Group, Cambridge, UK; email:*

### 7.4.1 Introduction

During flight test programmes structural response data may only be available in terms of accelerations, but relating these accelerations to stresses can be difficult without extensive analysis. Presented here is a method to quickly and accurately generate allowable acceleration levels to prevent fatigue failure. The method applies to lightly damped structures primarily excited at their fundamental mode such as antennae, radomes, and panels, but may be able to be conservatively extended if multiple modes exist.

The method relies on the structure primarily responding at its fundamental mode, and therefore that frequency can be used for the upwards crossing rate and also used to govern the relationship between acceleration and displacement. Furthermore, at the fundamental mode the relationship between displacement and detail stress can often be estimated based upon quasi-static considerations. Accurate understanding of the damping in the system is not required. Together these allow simplifications to be made to relate accelerations with stress and then fatigue damage.

Accuracy of the results is evaluated and quantified in this work, and the situations where acceptable accuracy achieved is defined. Finally, a nomogram is provided to aid the rapid calculation of allowable acceleration levels.

### 7.4.2 Discussion

If the structure in question is acting largely as a lightly damped oscillator with a dominant fundamental mode that provides the majority of response and if you are certain you understand that mode (say because the frequency is as predicted for that mode), then simplifications become available and the relevant parameters are:

- $f_n$ , fundamental mode frequency in [Hz],
- $\sigma/\delta$ , the relationship between displacement at the accelerometer position and detail peak stress in the part (may or may not be co-located) [MPa/m]
- L, the safe life [Hrs]
- $C_{safeRMS}$  [MPa] and b, the safe-life Basquin equation, for the detail in question ( $\sigma=C_{SAFE}N^b$ )
- $G_{RMS}$ , the RMS acceleration at sensor position [g]

$$\text{Leading to: } G_{RMS} = \left[ \frac{(2\pi f_n)^2}{9.8067} \right] \left( \frac{C_{SafeRMS}(3600 \cdot L \cdot f_n)^b}{\sigma/\delta} \right)$$

To aid quick calculation this equation is provided in Nomogram form in Figure 3.

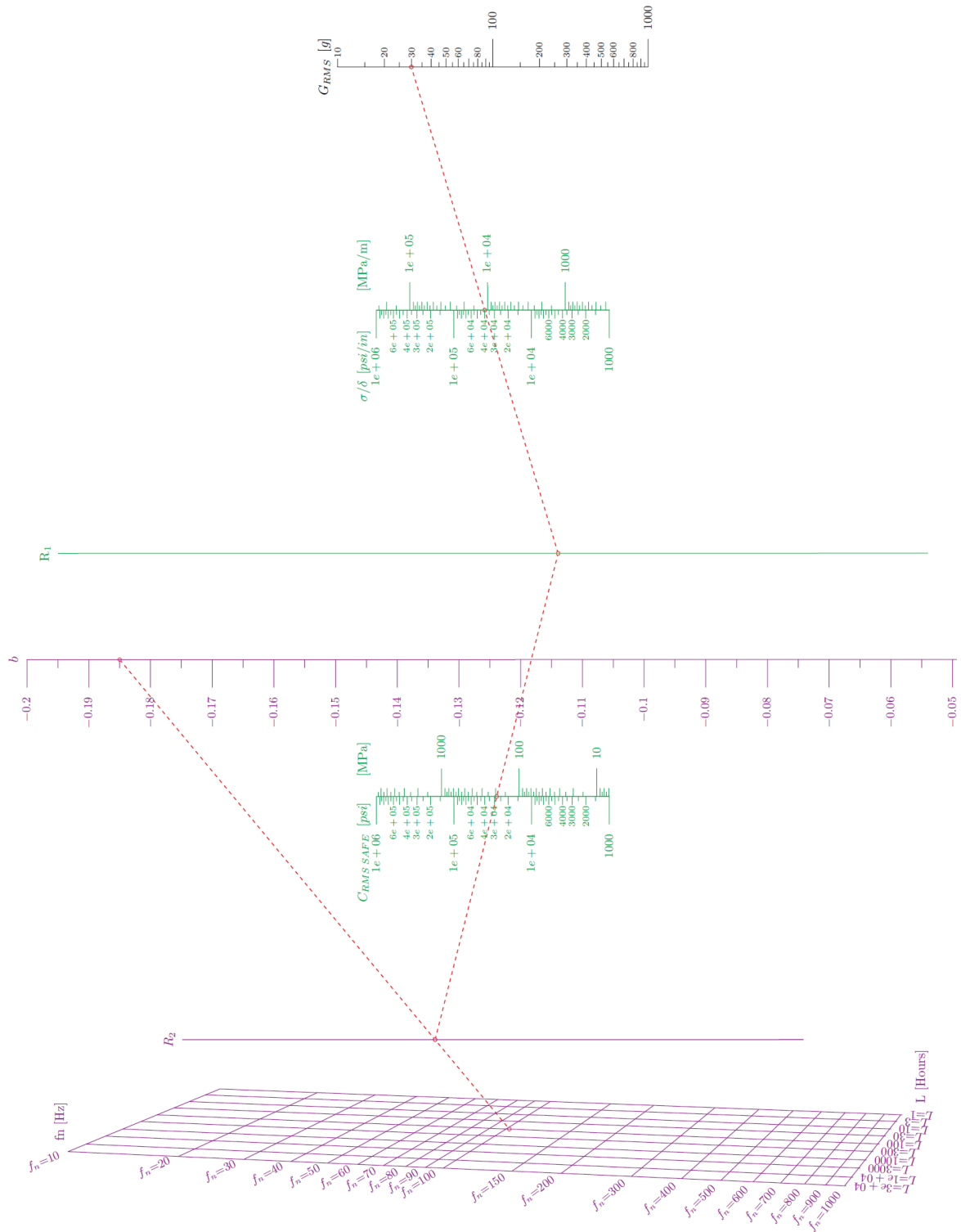


Figure 3: GRMS safe life nomogram

Example shown: Design Life  $L = 100$  [hours],  $f_n = 102$  [Hz],  $b = -0.185$ ,  $C_{RMS\_SAFE} = 194.3$  [MPa],  $\sigma/\delta = 1.086E4$  [MPa/m]

**Initial distribution**

1. ICAF2019
2. Contributors
3. Dstl KIS Athena



## Report documentation page

v5.0

\* Denotes a mandatory field

<b>1a. Report number: *</b>	DSTL/TR115301	<b>1b. Version number:</b>	Ver 1
<b>2 Date of publication: *</b>	01/05/2019	<b>3. Number of pages:</b>	ii + 64
<b>4a. Report UK protective marking: *</b>	UK OFFICIAL		
<b>4b. Report national caveats: *</b>	NONE		
<b>4c. Report descriptor: *</b>	NONE		
<b>5a. Title: *</b>	Review of aeronautical fatigue and structural integrity investigations in the UK during the period April 2017 - April 2019		
<b>5b. Title UK protective marking: *</b>	UK OFFICIAL		
<b>5c. Title national caveats: *</b>	NONE		
<b>5d. Title descriptor: *</b>	NONE		
<b>6. Authors: *</b>	Hallam, D.		
<b>7a. Abstract: *</b>	<p>This review is a summary of the aeronautical fatigue and structural integrity investigations carried out in the United Kingdom during the period April 2017 to April 2019. The review has been compiled for presentation at the 36th Conference of the International Committee on Aeronautical Fatigue and Structural Integrity (ICAF), to be held in Krakow, Poland in June 2019. The contributions generously provided by colleagues from within the aerospace industry and universities are gratefully acknowledged. The names on contributors and their affiliation are shown below the title of each item.</p>		
<b>7b. Abstract UK protective marking: *</b>	UK OFFICIAL		
<b>7c. Abstract national caveats: *</b>	NONE		
<b>7d. Abstract descriptor: *</b>	NONE		
<b>8. Keywords:</b>	Aeronautical fatigue, structural integrity, ICAF		

Please note: Unclassified, Restricted and Confidential markings can only be used where the report is prepared on behalf of an international defence organisation and the appropriate prefix (e.g. NATO) included in the marking.

# UK OFFICIAL

\* Denotes a mandatory field

<b>9. Name and address of publisher: *</b> Dstl Platform Systems Porton Down Salisbury Wilts SP4 0JQ	<b>10. Name and address of funding source:</b>
<b>11. Funding source contract:</b>	
<b>12. Dstl project number:</b>	
<b>13. Programme:</b>	
<b>14. Other report numbers:</b>	
<b>15a. Contract start date:</b>	<b>15b. Contract end date:</b>
<b>16. IP conditions for report: *</b>	
<b>17a. Patents:</b>	NO
<b>17b. Application number:</b>	
<b>18. Release authority role:</b>	

Guidance on completing the report documentation page can be found on the [Gov.UK website](https://www.gov.uk).

UK OFFICIAL

**UK OFFICIAL**

**THIS PAGE INTENTIONALLY LEFT BLANK**

**UK OFFICIAL**

**UK OFFICIAL**

This information is released for Defence purposes and whilst it does not attract a national Security Protective Marking, elements of the information may be of a sensitive nature and therefore the information is to be:

- Handled, used and transmitted with care.
- Basic precautions against accidental compromise, opportunist or deliberate attack are to be taken.
- Disposed of sensibly by destroying in a manner to make reconstruction unlikely.



**UK OFFICIAL**